Coherence in Energy Transfer and Photosynthesis

Aurélia Chenu[1] and Gregory D. Scholes[1,2]

[1]Department of Chemistry, University of Toronto, Toronto, Ontario M5S 3H6, Canada
[2]Department of Chemistry, Princeton University, Princeton, New Jersey 08544; email: gscholes@princeton.edu

Annu. Rev. Phys. Chem. 2015. 66:69–96

First published online as a Review in Advance on December 1, 2014

The *Annual Review of Physical Chemistry* is online at physchem.annualreviews.org

This article's doi: 10.1146/annurev-physchem-040214-121713

Keywords

light harvesting, exciton, quantum biology, two-dimensional electronic spectroscopy, process coherence, intermediate coupling regime, nonequilibrium processes

Abstract

Ultrafast energy transfer is used to transmit electronic excitation among the many molecules in photosynthetic antenna complexes. Recent experiments and theories have highlighted the role of coherent transfer in femtosecond studies of these proteins, suggesting the need for accurate dynamical models to capture the subtle characteristics of energy transfer mechanisms. Here we discuss how to think about coherence in light harvesting and electronic energy transfer. We review the various fundamental concepts of coherence, spanning from classical phenomena to the quantum superposition, and define coherence in electronic energy transfer. We describe the current status of experimental studies on light-harvesting complexes. Insights into the microscopic process are presented to highlight how and why this is a challenging problem to elucidate. We present an overview of the applicable dynamical theories to model energy transfer in the intermediate coupling regime.

1. INTRODUCTION

Coherent electronic energy transfer (EET): regime in which the system's unitary evolution (defined by the interchromophore coupling) competes with the dissipative evolution (determined by the system-bath coupling)

Förster theory: theory of electronic energy transfer applicable in the limit of very weak donor-acceptor electronic coupling in which transfer proceeds by (incoherent) hopping jumps

Plants contain sophisticated, regulated solar cells that are assembled with complexity at the molecular level. The photochemical energy transduction of photosynthesis starts with photoinitiated electron transfer reactions and proton transfer in photosystems embedded in the thylakoid membrane (**Figure 1*a***). The resulting stored transmembrane electrochemical potential drives further chemical transformations, called dark reactions, producing energy-rich molecules, such as sugars. All this starts when sunlight is absorbed by chromophores, such as chlorophyll, bound at high concentrations in light-harvesting proteins. As an example, **Figure 1*b*** shows the layout of chlorophyll molecules around the photosystem II reaction center. The excited state of a molecule such as chlorophyll is short lived compared to most biological processes, approximately 4 ns in vivo (1, 2). Nevertheless, faster processes ensue after chlorophyll absorbs light. Before the molecule returns to its electronic ground state, the electronic excitation must be harvested by electronic energy transfer (EET) that transmits the excitation energy to reaction centers by, as was first thought, a series of jumps (3–9).

All antennae complexes use EET to convert electronic excitation into charge separation with high efficiency (11). Quantum efficiencies—the probability of converting an absorbed photon into a charge-separated state—depend on the antenna size, excited-state lifetime of the chromophores used for light harvesting, arrangement of the chromophores, and light conditions. They are documented to be in the range 50–90%. For instance, the light harvesting to charge-separation efficiency is 84–90% for photosystem II of higher plants (12, 13). Characterizing the predominance of EET over donor fluorescence is of special importance for experimental studies. For a pair of photosynthetic chromophores, the Förster radius—the characteristic distance by which the EET efficiency drops by 50%—is estimated to be quite large, 60–100 Å, showing the effectiveness of these chromophores at mediating rapid EET (14, 15). Researchers are seeking design principles for efficient light-harvesting complexes (7), and because photosynthetic complexes have diversified

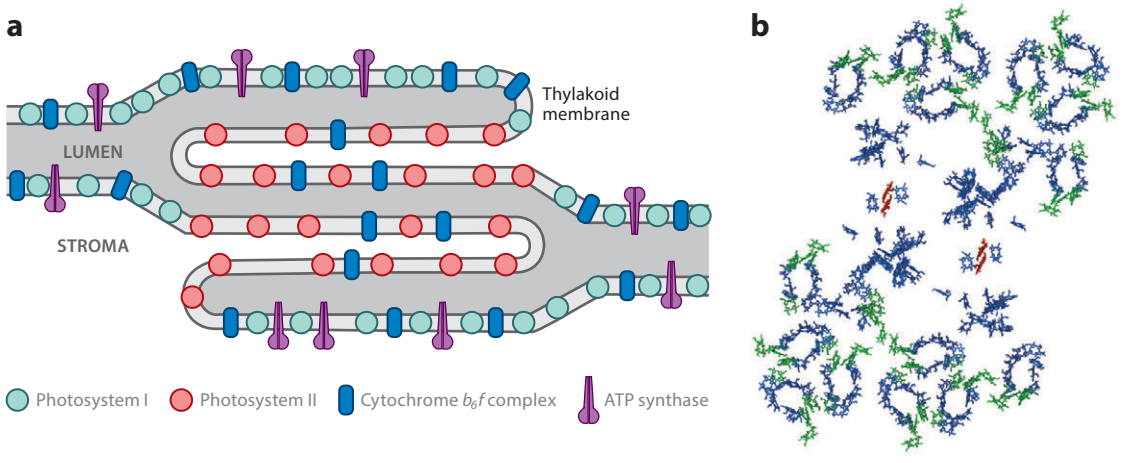

Figure 1

(*a*) The spatial distribution of light-harvesting complexes embedded in the thylakoid membrane viewed in cross section. (*b*) Model of the photosystem II supercomplex C2S2M2 from higher plants viewed in the plane of the thylakoid membrane, showing the organization of chlorophylls bound in these proteins. Chlorophyll *a* is shown in green, and chlorophyll *b* is in blue. The special pair of chlorophylls in the photosystem II reaction center, which launches the electron transfer, is shown in red. Figure reproduced from Reference 10 with permission from Elsevier.

and optimized over the past three billion years, they are clearly good models. For example, Vos et al. (16) have shown that in purple photosynthetic bacteria, excitation can migrate among ~1,000 bacteriochlorophylls—in other words, approximately 25 reaction centers are within the radius of excitation energy transport.

Underpinning these expansive perspectives are mechanistic aspects of light harvesting and energy transfer that have long been of interest in physical chemistry. The questions if, how, and why coherence assists the dynamics of light harvesting have recently generated great interest (17–19). In other words, is the incoherent hopping model, in which excitation energy jumps randomly from molecule to molecule, a sufficient mechanistic description of light harvesting? The topic of coherence in EET has been highlighted by recent experiments (20–22), described below, that have motivated extraordinary developments in theories for EET. Partly because the word coherence has various connotations and contexts, the meaning and consequences of coherent EET (coherent transfer as opposed to incoherent hopping jumps) as well as associated issues and concepts can easily be misconceived. A primary goal of this review is to document the notion of coherence and discuss these issues. We try to clearly define coherence with respect to energy transfer and provide context by presenting concepts of coherence in Section 3.

Why are similar questions of coherent transfer for electron transfer not debated, given that the underlying assumptions for Marcus theory are not too different from those of the Förster theory of incoherent EET? One major difference between the two is that in EET, the interchromophore electronic coupling covers a vast range. It can be very small compared to the absorption line widths (less than a few wave numbers), in which case Förster theory works well, or it can be several hundreds of wave numbers, in which case the electronic states are strongly perturbed and excitation energy flows among delocalized states. All these situations are found in photosynthetic light-harvesting complexes, which is partly why they are so fascinating to study.

As a reference point, here we remind the reader about the key elements of the Förster theory for (incoherent) EET (23–26). On the basis of second-order perturbation theory in the electronic coupling between the donor (*D*) and acceptor (*A*), an intuitive and quantitative expression for the energy transfer rate k was derived in terms of the electronic coupling V [screened by the polarizable medium (27, 28)] that exchanges excitation between the molecules and a spectral overlap $I(\varepsilon_D, \varepsilon_A, \varepsilon)$ that ensures energy conservation when the donor de-excites and the acceptor synchronously gains excitation:

$$k = \frac{2\pi}{\hbar} |V|^2 \int_0^\infty d\varepsilon \; I(\varepsilon_D, \varepsilon_A, \varepsilon), \tag{1}$$

where ε denotes the transition energy (see 23 for details). Unlike the usual Förster spectral overlap, this spectral overlap, $I(\varepsilon_D, \varepsilon_A, \varepsilon) = f(\varepsilon_D, \varepsilon)a(\varepsilon_A, \varepsilon)$, is defined as a product of the area-normalized donor fluorescence spectrum f and the area-normalized acceptor absorption spectrum a. Basically, the rate of EET from the electronically excited donor to the ground-state acceptor depends on the coupling strength between the de-excitation of the donor and excitation of the acceptor, and therefore their spectral properties. To emphasize how spectroscopy distinguishes between intramolecular vibronic transitions—typically large frequencies compared to the homogeneous line width—and line broadening that comes from interactions of the chromophores with stochastic fluctuations in the environment, we explicitly write the possible vibronic transitions on the donor and acceptor hidden in Equation 1 from their occupation probabilities P at thermal equilibrium and their associated Franck-Condon factors $\langle \chi^{(e)} | \chi^{(g)} \rangle$:

$$k = \frac{2\pi}{\hbar} \sum_{i,j,m,n} P_j P_m \left| V \left\langle \chi_j^{(e)} \middle| \chi_i^{(g)} \right\rangle \left\langle \chi_m^{(g)} \middle| \chi_n^{(e)} \right\rangle \right|^2 \int_0^\infty d\varepsilon \; I_0(\varepsilon_D + \varepsilon_j - \varepsilon_i, \varepsilon_A + \varepsilon_m - \varepsilon_n, \varepsilon), \tag{2}$$

where i and j label vibrational levels (with energies ε_i and ε_j) on the ground and excited state of D, m and n label those on A, and I_0 is the spectral overlap of two homogeneously broadened lineshapes.

This equation shows the prominent, often crucial, role played by vibronic transitions for energy matching between de-excitation of the donor and excitation of the acceptor. Numerous illustrative examples can be found in Reference 29. Accounting for intramolecular modes in terms of their realistic spectroscopic properties is an important facet of EET that deserves deeper attention in theories for coherent EET.

Exciton/steady-state electronic coherence: delocalized electronic excited states comprising a superposition of excitations at different molecular sites that result from interchromophore electronic coupling and appear as off-diagonal elements in the site-basis density matrix

2. PHOTOSYNTHESIS: HOW IS COHERENCE RELEVANT?

2.1. The Electronic Couplings Range from Small to Large

Electronic coupling between chromophores (30, 31) leads to delocalized excited states—excitons. Molecular excitons are delocalized electronic excited states comprising a superposition of excitations at different molecular sites (32–36). Correspondingly, coupling is responsible for coherence (i.e., off-diagonal elements in the site-basis density matrix) among sites. Because exciton states manifest in the steady-state spectrum, we term this superposition steady-state electronic coherence. As reviewed previously (23, 37), excitons (or, equivalently, these steady-state electronic coherences) are important for light harvesting in photosynthesis.

The main origin of the electronic interaction between an excited molecule and a nearby ground-state molecule is the long-range Coulomb interaction between transition densities (30), modified by the interaction of the optical dielectric properties of the medium (screening). Coupling between chromophores in the vast majority of light-harvesting complexes takes values ranging across three orders of magnitude: from $\sim$0.5 cm^{-1} up to $\sim$500 cm^{-1} after screening is taken into account (27, 28, 38).

Electronic coupling is decided by the relative positions and orientation of the chromophores in the protein scaffold of light-harvesting complexes. Nature has evolved many different chromophore organizations, reflected in the diversity of light-harvesting complexes. Even within each family of light-harvesting complexes, nature continues to manage electronic couplings through structural modifications that are genetically encoded. A well-established example is the normal versus low-light forms of the LH2 light-harvesting complex from some purple bacteria (39).

Recently, a remarkable variation within a family of light-harvesting structures has been discovered for the *Cryptophyceae* (cryptophyte algae) (40). **Figure 2** shows two different ways that electronic coupling is controlled between the pair of bilin chromophores at the center of the cryptophyte light-harvesting complexes: through the orientation of the bilins and through the insertion of an amino acid. The most common structure appears to be the closed structure, in which the large β-subunits are sandwiched together so that the central bilin molecules approach each other to within a few angstroms. Whereas the separation between these bilins is very similar for PC645 and PE545, the orientation is slightly different, yet that difference is enough to change the electronic coupling substantially. An even more drastic modification is found in the genus *Hemiselmis* (PC612 and PE555), where the insertion of a single amino acid in the small α-subunits leads to a steric clash that rotates and separates the β-subunits, thereby rendering the electronic coupling between the central pair of bilins very small. By expressing this gene for the α-subunits, the organism switches off the strong exciton effects that influence the function of PC645 and PE545.

This switching off of the exciton coupling is especially interesting in comparison to the related subunits of phycobilisomes, for which exciton effects appear to be significant (42–44). In a broader context, genes control protein structure and that structure in turn decides the electronic

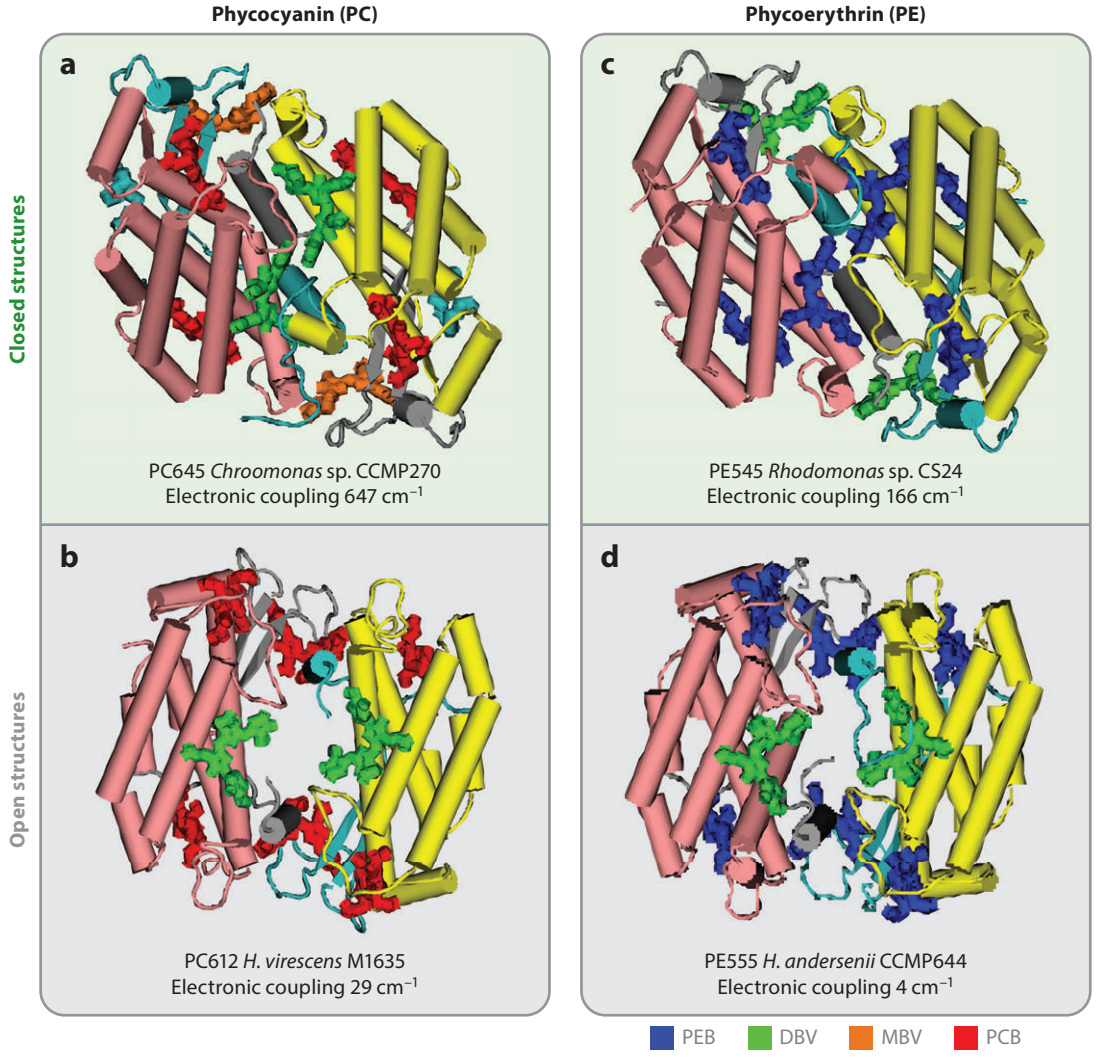

Figure 2

Structures of four representative phycobiliproteins from cryptophyte algae (40, 41): two phycocyanin light-harvesting complexes, (*a*) PC645 and (*b*) PC612, and two phycoerythrin light-harvesting complexes, (*c*) PE545 and (*d*) PE555. PC645 and PE545 (*top row*) are examples of closed structures, characterized by a large electronic coupling between the chromophores in the indicated central dimer of bilins. PC612 and PE555 (*bottom row*) are examples of open structures, in which the electronic coupling is weak. The large β-subunits are colored pink and yellow, and the small α-subunits are colored cyan and gray. Abbreviations: DBV, 15,16-dihydrobiliverdin; MBV, mesobiliverdin; PCB, phycocyanobilin; PEB, phycoerythrobilin.

Hamiltonian underpinning light-harvesting function. Strong exciton dimers that evolved in these cyanobacterial phycobilisome antenna complexes were preserved in red algae (endosymbionts of cyanobacteria) but were re-engineered twice by cryptophytes (endosymbionts of red algae) in the open and closed phycobiliproteins shown in **Figure 2** (45). We do not really know what specific role these exciton dimers play in light harvesting. The calculations of PC645 dynamics reported by Huo & Coker (46) imply that their main roles are perhaps to broaden the spectral absorption cross section and to set up an energy funnel from the center of the protein to its periphery.

The light-harvesting complex of purple photosynthetic bacteria, LH2, presents a model example of strong electronic coupling. A dense, ordered arrangement of bacteriochlorophylls in the so-called B850 ring allows the chromophores to work cooperatively in light harvesting (39). Excitonic states are formed, leading to a red shift of the absorption spectrum and delocalization of excitation energy, clearly distinguishing the bacteriochlorophylls in the B850 ring from those in the B800 ring in which excitation tends to be localized. The result is an incredible increase in the energy-funneling rate from the B800 to B850 ring, faster by an order of magnitude than predictions based on localized states (4, 47).

It is remarkable how photosynthetic organisms have evolved such a range of aggregation states and electronic couplings and, furthermore, incredible that still they avoid concentration quenching. Concentration quenching, originally observed in solutions of organic dyes, describes the rapid decrease in quantum yield when a fluorophore is in high concentrations, such that certain aggregates are formed. The fluorescence emission of dissolved chlorophyll *a* is strongly quenched at a concentration of 0.1 M (48, 49). In light-harvesting complexes, chromophores are packed at higher concentration, but they completely avoid concentration quenching. For example, the chlorophyll in the light-harvesting complexes of plants and green algae (LHCII) has an effective concentration of 0.25 M (50), yet its excited-state lifetime is hardly changed compared to that of monomeric chlorophyll *a*. Aggregated bacteriochlorophylls in the light-harvesting organelles of green sulfur bacteria, called chlorosomes, are present at a concentration of ~2 M (51). These observations remind us of the many factors to consider in the design of light-harvesting systems, including those such as concentration quenching that are currently neglected by theories for EET.

2.2. System-Bath Interactions in Proteins May Be Fine-Tuned

Line broadening matters significantly, even at the level of Förster theory, because it determines the magnitude of the spectral overlap integral shown in Equation 1, $\int_0^\infty d\varepsilon f(\varepsilon_D, \varepsilon)a(\varepsilon_A, \varepsilon)$. Even for perfectly overlapped donor emission and acceptor absorption lineshapes, the spectral overlap is not unity—except when $f(\varepsilon_D, \varepsilon)$ and $a(\varepsilon_A, \varepsilon)$ are delta functions. This is easily demonstrated by considering rectangular lineshapes of energy width w. The ordinate of each area-normalized spectrum is then $1/w$, and the overlap integral is $(1/w)^2 w = 1/w$ (i.e., the spectral overlap diminishes as the inverse of the line width). In models beyond Förster theory, it is essential to know and to account for many more details about the bath, especially the timescales of fluctuations that produce line broadening. Emphasizing this point was an important contribution of the Fleming group (18, 52), and it is discussed further in Section 5.

The influence of the environment around the chromophores in light-harvesting complexes is partly revealed by the Stokes shift—the energy difference between the absorption and fluorescence maxima. According to models for line broadening in molecules in solution, the Stokes shift measures two times the reorganization energy λ, which tells us how strongly the electronic transitions of the chromophores are coupled to the environment. The Stokes shift of chlorophyll *a* in LHCII is approximately 110 cm^{-1} (53). It is significantly reduced compared to that of chlorophyll *a* in solution, in which it ranges from 135 to 200 cm^{-1}, depending on the solvent polarity (54), which suggests that reorganization energies in light-harvesting complexes have evolved to be smaller than those in solution environments.

2.3. How Excitons and Coherent Transfer Matter

The reorganization energy, which characterizes the coupling between chromophore electronic transitions and the environment in photosynthetic proteins, is approximately 50–100 cm^{-1}, and

the expanse of electronic coupling strengths ranges between ~0.5 and 500 cm^{-1}. Whereas the first interaction is responsible for dissipative evolution, the second contributes to unitary evolution. Because the two different couplings are in the same range, the two opposite evolution processes compete (55): This corresponds to coherent EET (coherent in contrast to Förster incoherent EET), in which excitation delocalization and superposition between the molecular sites (steady-state electronic coherence) are robust to the dissipating effect of the bath fluctuations on the individual chromophores.

The recent experiments, described in Section 4, that reveal long-lived coherent superpositions of eigenstates after femtosecond-pulse excitation have initiated much discussion about what coherent energy transfer is and what it means—for example, does it enable energy to move faster and further? After much thought, we believe the answers are simple: Coherence of the process, which maintains the superposition of sites on a timescale during which EET occurs, matters, and it does indeed accompany fast energy transfer. Such a firm statement is based on the following reasoning and working definition of coherent energy transfer.

Starting with Förster theory, the rate of energy transfer is directly proportional to $|V|^2$; that is, it rises quadratically with the electronic coupling when it is very small compared to the reorganization energy of the environment, λ (**Figure 3**). At the other limit, when V is very large, the dynamics convert to relaxation between exciton levels—as modeled by Redfield theory. We exclude radiationless transitions that can sometimes make this relaxation very fast (56) and concentrate only on bath-mediated relaxation for consistency. As the exciton splitting increases, the relaxation rate diminishes because the electronic gap is not bridged by bath fluctuations. Somewhere in the middle of these two limiting cases is the fastest energy transfer, as elucidated for different parameters in References 57 and 58. We define this regime as coherent EET, recognizing that there is a range of factors contributing to maintain the coherent superposition of sites as V increases. An increase in the electronic coupling means larger delocalization (i.e., a steady-state electronic coherence with a larger amplitude). In the intermediate regime, the exciton (site coherence) is furthermore retained

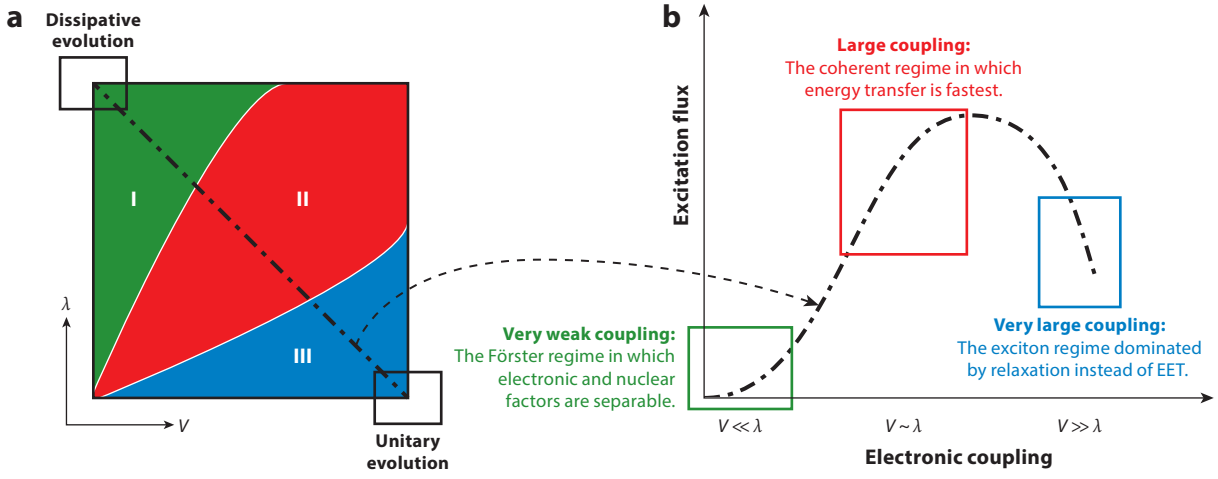

Figure 3

(*a*) The regimes of electronic energy transfer (EET), specifically (*I*) incoherent Förster transfer, (*II*) the intermediate coupling regime (coherent EET), and (*III*) the Redfield excitonic regime. (*b*) Depiction of the dependence of the rate of a general excitation energy transfer process on the electronic coupling V for a representative system-bath interaction λ. Figure inspired by Reference 59.

while excitation is transferred, and the rate of energy transfer becomes larger (see **Figure 3**). Therefore, fast energy transfer goes hand in hand with coherent EET.

In the limit of very small or large electronic coupling, the commonly used second-order perturbative methods of Förster or Redfield theory, respectively, work quite well. However, they are not appropriate in the intermediate regime, as clearly shown by the Fleming group (18, 52, 60, 61), particularly because they fail to capture dynamical aspects of the bath that become relevant to the evolution (62). In this intermediate regime, the timescale characterizing the bath relaxation is on the order of the transfer process, and the Born approximation is no longer valid. The electronic and nuclear factors cannot be factorized, and nonequilibrium phonons can play a role in the dynamics (18, 63). Simple path interferences can be identified, and bath correlations come into play (64, 65). In that case, nonperturbative numerical methods for accurately computing quantum dissipative dynamics, such as hierarchical equations of motion (HEOMs) (52, 66) or path-integral approaches (61, 67, 68), are suitable, although methods using a polaron transformation have also proven to be adequate (69–72). We discuss these theories in Section 5.

Classical coherence: temporal (spatial) coherence resulting from temporal (spatial) correlation and spectral coherence characterized by a particular phase relationship between the different spectral components

State coherence: superposition of states resulting in a well-defined phase relationship between the states

3. HOW TO THINK ABOUT COHERENCE

The previous section demonstrates that the word coherence can take different meanings; for example, in the context of photosynthesis, electronic coherence denotes a superposition of sites, whereas coherent EET characterizes the competition between dissipative and free evolution. Although a coherent state is a well-defined, unambiguous concept in the quantum optics community, different definitions of coherence are being used in the field of physical chemistry. In the hopes of avoiding further misconceptions, we dedicate this section to the general concepts of coherence. We present the main classical coherences, give the quantum-mechanical definition of state coherence, and emphasize how it is different from the coherence of the process.

3.1. Classical Coherence: Temporal, Spatial, and Spectral Correlation

Classically, the concept of coherence is fundamental in all fields dealing with fluctuating quantities, and it is tied with that of correlation, often revealed experimentally from an interference pattern. Three basic types of classical coherence can arise from temporal, spatial, and spectral correlation, and these need to be distinguished. Temporal and spatial coherence each provide a pattern that improves our ability to predict or extrapolate data on the basis of previous observations. These notions are entirely classical and have applications in a wide variety of fields, from neurology to meteorology and fluid mechanics.

Within the framework of probability theory, the degree of coherence between two random variables X and Y is quantified by the correlation coefficient ρ:

$$\rho = \frac{R_{XY}}{\sqrt{R_{XX}\,R_{YY}}}, \tag{3}$$

where $R_{XY} = \int\int xy^{*} f_{XY}(x, y)\mathrm{d}x\ \mathrm{d}y$ denotes the expectation value of the joint probability density f_{XY} (73). Here, we present the concept of coherence based on analysis of the electromagnetic field. This allows us to use the extensive work of Glauber (74), who described coherent properties beyond the classical theory. Classical coherences are characterized by the first-order correlation function

$$G^{(1)}(r_1, t_1; r_2, t_2) = \langle E^{(-)}(r_1, t_1)E^{(+)}(r_2, t_2)\rangle, \tag{4}$$

where $E^{(+)}[E^{(-)}]$ denotes the positive (negative) frequency of the field, and the terms in angled brackets denote a time average. This reduces to the correlation coefficient ρ after normalization.

When two fields are entirely correlated, the interference fringes have the maximum intensity, and the correlation function factorizes. If the waves are correlated only over a limited time (or region in space), it is convenient to define the coherence time (length) over which this criterion holds and for which the waves can be considered coherent.

For stationary fields, the ergodic property results in an equivalence between time and space averages, so the Wiener-Khinchin theorem gives the first-order correlation function as the Fourier transform of the spectral density $S(\omega)$:

$$G^{(1)}(\tau) \equiv G^{(1)}(r, t; r, (t+\tau)) = \lim_{T\to\infty} \frac{1}{T} \int_0^T S(\omega) e^{-i\omega\tau} d\omega. \quad (5)$$

The coherence time is then defined as the inverse of the full width at half maximum of the spectral bandwidth, $\tau_c = 1/\Delta\omega$ (75). Importantly, the coherence time, which characterizes temporal coherence, is fully defined from the spectral distribution (i.e., from the amplitude of the Fourier coefficients). There is no notion of the spectral components' relative phases.

Figure 4 schematically illustrates the difference between temporal and spectral coherence. We present states of light that share the same coherence time because of similar spectral lineshapes but differ in their spectral coherences because of different relative phases of the spectral components. For the purpose of illustration, we consider states of light composed by continuous waves. Continuous waves are modeled as monochromatic coherent states in quantum optics and exhibit quantum coherence as a superposition of photon-number states. The relative phases of different spectral components define both the spectral and quantum coherence. For example, in state A, a linear phase relationship results in a pulse characterized by both spectral and quantum coherence, whereas in state B a fixed, but arbitrary, phase between the components conserves the quantum coherence but removes the spectral coherence to produce an electric field that is chaotic in time. In state C, the phase is arbitrary (no spectral coherence) and unknown; then an average over the random phases removes the quantum coherence and leads to an expectation value of zero for the electrical field (typically, this state would be representative of thermal light). Although state B could be defined as incoherent in the classical sense of the term because of the chaotic behavior of its electric field in the time domain, it can still exhibit coherence in the quantum-mechanical definition (given hereafter), specifically as a superposition of eigenstates.

3.2. Coherence in Quantum Mechanics

In the context of EET, molecular excitons (superpositions of electronically excited states) are certainly important, but they are not the only examples of the coherence possible in energy transfer dynamics. The challenge is to conceptualize coherence. Superposition is a concept that has special significance in quantum mechanics, and it is responsible for state coherence. This is a (static) property of the system and is therefore to be distinguished from the system's dynamical properties, such as the coherence of the process. Here we discuss these concepts.

3.2.1. State coherence. In quantum mechanics, coherence stems from the superposition principle and the possibility of the system being in a linear superposition of individual realizations. Individual realization can refer to individual states or evolution pathways. Each component represents only a partial amplitude contributing to the total probability upon measurement. The superposition imposes a well-defined phase relationship responsible for interferences in the partial probability amplitudes in such a way that the outcome of an experiment (total amplitude) is different from the sum of measurements performed on the individual realizations. Any attempt to determine the state of the system or the path through which it evolved destroys the well-defined

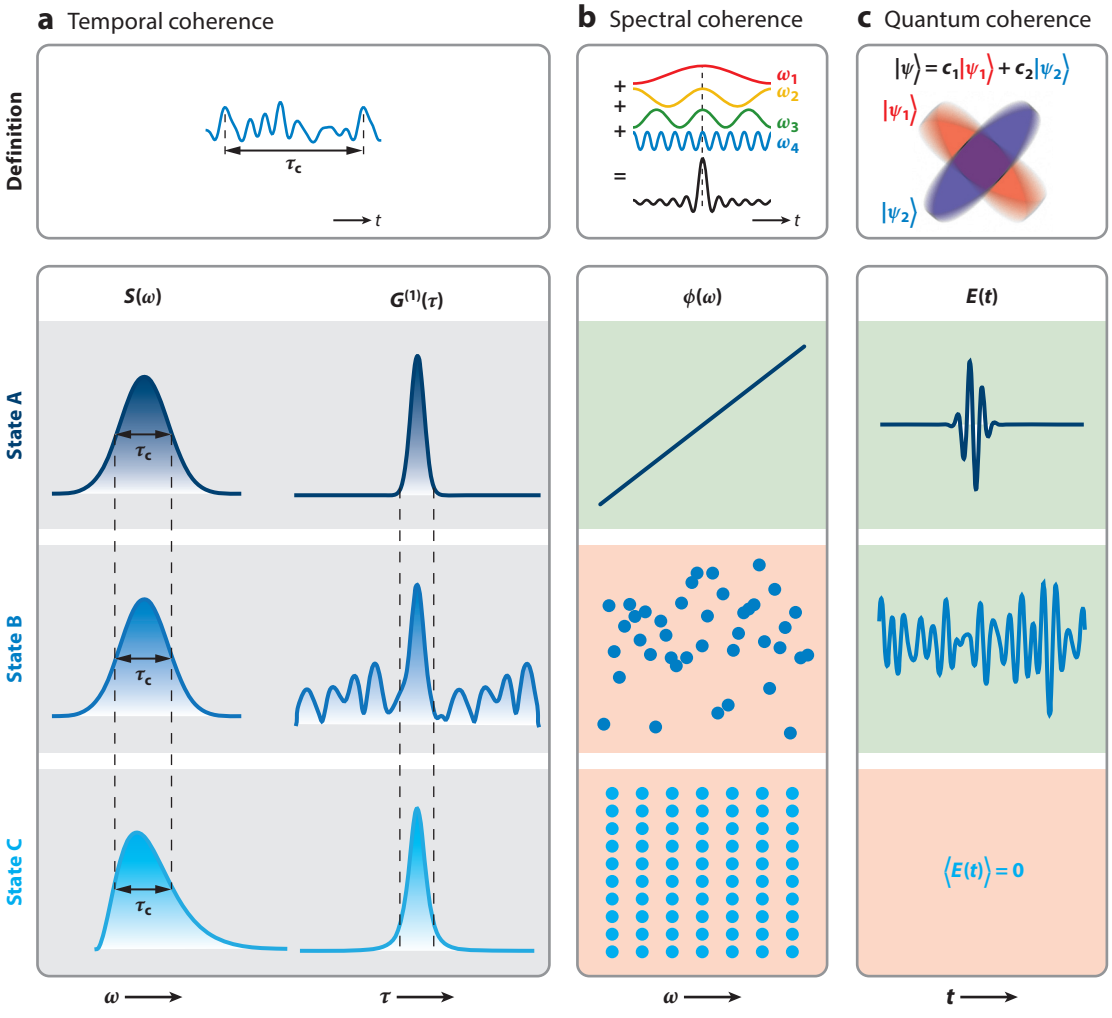

Figure 4

Schematic representations of three different kinds of coherence—(*a*) temporal, (*b*) spectral, and (c) quantum—illustrated for different states of light. All states of light shown have similar temporal coherence and coherence time τ_c because of similar spectral lineshapes. State A is characterized by a linear phase relationship between the spectral components and illustrates a pulsed light with both spectral and quantum coherence. State B is formed by a mixture of continuous waves with a fixed but arbitrary phase relationship that removes the spectral coherence. It can still contain quantum coherence as a superposition of photon-number states. In state C, the phase of the continuous waves is unknown (no spectral coherence). Averaging over the random phases removes the quantum coherence between the photon-number states. This state is representative of thermal light. The green (red) background emphasizes the coherent (incoherent) character. *E* denotes the electrical field, *S* the spectral lineshape, $G^{(1)}$ the first-order correlation function (Equation 4), and ϕ the phase of the different spectral components ω.

phase relationship and alters the system, making all the phases of the partial amplitudes random relative to each other and removing all interference effects in the average amplitude.

It is relevant to recall the differentiation between a pure state and a mixed state. For the purpose of illustration, let us consider an observable $\hat{O}$ with eigenvectors $|O_\alpha\rangle$ and eigenvalues o_α. We denote the partial probability amplitudes as $p_n(o_\alpha) \equiv |\langle O_\alpha|\psi_n\rangle|^2$. For a pure

state, the density matrix can be written as $\rho = \sum_n |c_n|^2 \, |\psi_n\rangle \, \langle\psi_n| + \sum_{n\neq m} c_n c_m^* \, |\psi_n\rangle \, \langle\psi_m|$. The probability of measuring the eigenvalue o_α is the square of the sum of the partial probability: $P(o_\alpha) \equiv \langle O_\alpha|\rho|O_\alpha\rangle = \sum_n |c_n|^2 \, p_n(o_\alpha) + \sum_{n\neq m} c_n c_m^* \langle O_\alpha|\psi_n\rangle \, \langle\psi_m| \, O_\alpha\rangle$. This is different from a measurement performed on a mixed state, $\rho = \sum_n |c_n|^2 \, |\psi_n\rangle\langle\psi_n|$, where the outcome of the measurement is simply the sum of the different probabilities without any interference: $P(o_\alpha) = \sum_n |c_n|^2 \, p_n(o_\alpha)$. In the first case, because the off-diagonal terms $|\psi_n\rangle \, \langle\psi_m|$ are responsible for the interferences in the final outcome, they are defined as coherent terms. We note, however, that this definition is basis dependent and that it is always possible to find a basis in which ρ is diagonal. Therefore, one should be careful before giving any physical interpretation to the quantum coherence defined as an off-diagonal element of the density matrix.

Process coherence: interplay between dissipative and free evolution dynamics

Interestingly, the classical definition of coherence (through the first-order correlation function) resembles the quantum-mechanical definition (through the superposition principle). Let us take, for example, a broadband electromagnetic field, which can be $E = \sum_\omega c_\omega E_\omega$, where the ω subscript here denotes the frequency. Using this spectral decomposition, one can discuss Young's double-slit experiment in which the electric field plays the role of the probability amplitude. When there is no attempt to determine through which slit the light passes, the fields (and not their intensities) radiated through the two slits must be added to determine the measured outcome: $|E|^2 = \sum_\omega |c_\omega|^2 \, |E_\omega|^2 + \sum_{\omega\neq\omega'} c_\omega c_{\omega'}^* \langle E_{\omega'}^* E_\omega\rangle$. Clearly, it is the superposition of various (spectral) components that is responsible for the interference pattern.

3.2.2. Process coherence. In the context of EET, it is important to distinguish between state coherence, defined from the superposition principle as presented above, and process coherence, as clearly described by Kassal et al. (76) and discussed in Reference 77. Section 2 defines the intermediate coupling regime as coherent EET, with the term coherent qualifying the process and characterizing the competition between the unitary and dissipative evolution of the system (59, 76), determined, in photosynthetic complexes, by interchromophore electronic interactions and by the coupling to the bath, respectively. In this context, the lifetime of the beats after the ultrafast coherent excitation of the light-harvesting complexes indicates how long, when excited coherently, the process maintains the superposition of eigenstates (state coherence). Therefore, although the experiments use coherent laser excitations that differ from natural light conditions, recognized as generating different initial excited states in particular theoretical models (78–80), they are fundamental to assess the properties of the system, such as the electronic coupling strength relative to that of the system-bath coupling. As such, they allow us to qualify the regimes of EET. The coherent regime discussed below is a property of the system and therefore occurs regardless of the excitation conditions.

4. ELECTRONIC, VIBRATIONAL, AND VIBRONIC COHERENCE

Here we give an overview of the experimental observations of coherence as superpositions of states. Combined with theoretical analysis, recent spectroscopic techniques have uncovered new details of coherence in energy transfer.

4.1. Background

Ultrafast spectroscopy has a well-established and important history in the context of photosynthesis. Structural models provide the foundation for understanding photosynthesis, whereas time-resolved spectroscopy was seen early on as a way of resolving the function of the photosynthetic machinery, step by step (6, 81). Vast amounts of information have been learned about light

harvesting, in particular using femtosecond laser experiments. Most recently, two-dimensional (2D) electronic spectroscopy has revealed new details (82–85), especially concerning the dynamics of molecular excitons (9, 17, 20, 86). Current research is trying to better decode the information presented in 2D electronic spectra and to work out the significance of those observations for light harvesting.

Femtosecond laser pulses with spectra that span vibrational level spacings can photoexcite superpositions of vibrational levels (and rotational levels for gas phase molecules) in the ground and excited states of chromophores (87). The time evolution of those superpositions, or wave packets, is detected by a probe pulse as coherent modulations of the signal amplitude as a function of time after the pump pulse (88–91). In the context of photosynthesis, Vos and coworkers (92, 93) detected coherent vibrational motion in studies of reaction centers isolated from purple bacteria. At the time, this discovery was surprising because it was thought that the thousands of atoms in the protein binding the chromophores would expedite the decoherence and dissipation of the vibrational wave packets. Later, coherent oscillations (with frequencies $\sim$100 cm^{-1}) were found in other studies of photosynthetic proteins, for example, LH1 and LH2 light-harvesting complexes from purple bacteria (94–96).

In recent work, our group used broadband femtosecond pump-probe spectroscopy to study a photosynthetic cryptophyte antenna complex, PC577, isolated from *Hemiselmis pacifica* (CCMP 706) (97). The sample was dispersed in aqueous buffer and maintained at ambient temperature. This light-harvesting complex is very similar in structure to PC612, shown in **Figure 2**, with a cryptophyte open structure without strong exciton coupling in the central chromophore dimer. It serves to illustrate coherent oscillations from vibrational wave packets in pump-probe data.

Figure 5*a* shows the absorption spectrum of PC577 and the structure of the protein. The pump and probe laser pulses are identical in spectrum (covering the absorption spectrum) and duration ($\sim$15 fs). The change in probe transmission as a function of the pump-probe time delay contains picosecond decay components, particularly on the blue side of the absorption spectrum. These decays reveal the energy transfer dynamics. When those exponential amplitude changes are subtracted from the data, the coherent oscillations in the signal amplitude are easily seen (**Figure 5*b***). Several vibrational frequencies were distinguished (97), and analysis of vibrational wave-packet dynamics showed that the oscillations are contributed by superpositions of levels in the excited electronic state. Whereas experiments often produce coherent vibrational motion on the ground electronic state (98, 99), excitation with broadband pulses that cover the entire absorption spectrum produces excited-state wave packets (100, 101).

The evidence for excited-state vibrations is provided by the node seen at a probe wavelength of $\sim$640 nm in **Figure 5*b***, lining up with the peak of the fluorescence spectrum. The wave packets pass through the minimum of each vibrational potential—a point probed at the free energy minimum that is resonant with the probe wavelength of 640 nm—twice per period of oscillation, not once like at the turning points (e.g., see 102, figure 2*a*). Therefore, the fundamental oscillation frequency is not detected at 640 nm, and instead a node is seen.

4.2. Two-Dimensional Spectroscopy and Vibronic Coherence

Two-dimensional electronic spectroscopy (2DES) is a femtosecond pump-probe technique that resolves both pump and probe frequencies. It thus cross-correlates the visible-light absorption spectrum, which enables related excitonic states to be identified by cross peaks (17, 82, 85, 103–106). 2DES is similar to transient absorption spectroscopy; however, two excitation pulses are used cooperatively to excite the sample, followed by a third probe pulse, which interacts with the sample after the pump-probe time delay, causing a four-wave mixing signal to radiate. By Fourier

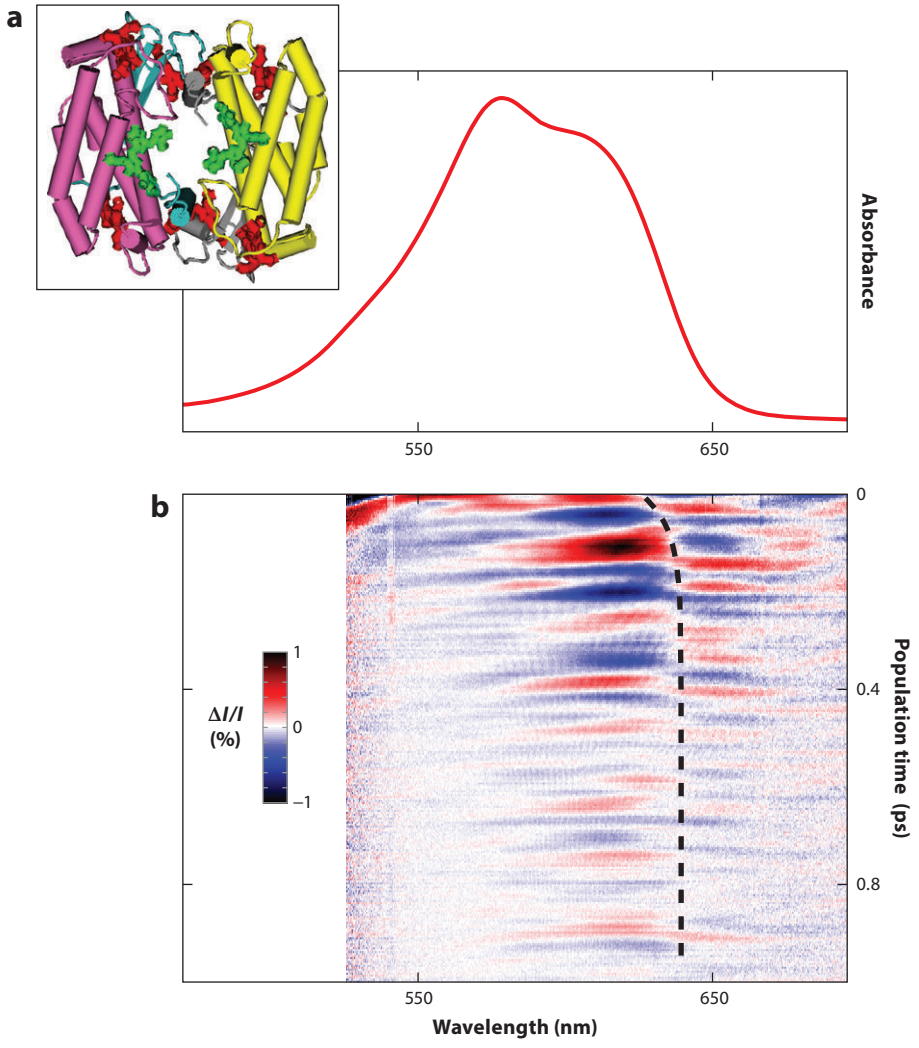

Figure 5

(*a*) The absorption spectrum of the light-harvesting complex PC577 from the cryptophyte *Hemiselmis pacifica* (CCMP 706) and the structure of the protein. (*b*) The transient absorption signal of PC577, showing the coherent oscillations during the first picosecond after excitation. The background decay features were independently removed at each probe wavelength to highlight the coherent oscillations as a function of the probe wavelength and pump-probe delay time. A sharp node is seen at approximately 640 nm (*black dashed line*).

transforming the signal amplitude with respect to the delay between the two excitation pulses, one can obtain the excitation frequency axis for a given time delay. The probe axis is frequency resolved by dispersing the signal in the detector, similar to normal pump-probe methods. Inhomogeneous broadening in the absorption lineshape elongates the spectrum in the diagonal dimension. Homogeneous broadening depends on fluctuating system-bath interactions and elongates the spectra in the antidiagonal direction. Thus, changes in the lineshape of the 2D spectrum indicate solvation dynamics and spectral diffusion.

As we wrote elsewhere (86), a basic understanding of a 2D spectrum can be achieved by treating one axis as the emission axis and the other as the excitation axis. In the corresponding 2D map, signals along the diagonal represent transitions in which the excitation and emission frequency are the same. Off-diagonal signals correspond to transitions in which the excitation and emission frequencies are different and represent correlations between the corresponding transitions absorbing and emitting at those frequencies. A 2D spectrum is a map correlating excitation and emission frequencies at a given probe delay. **Figure 6*a*** shows a sample 2D spectrum

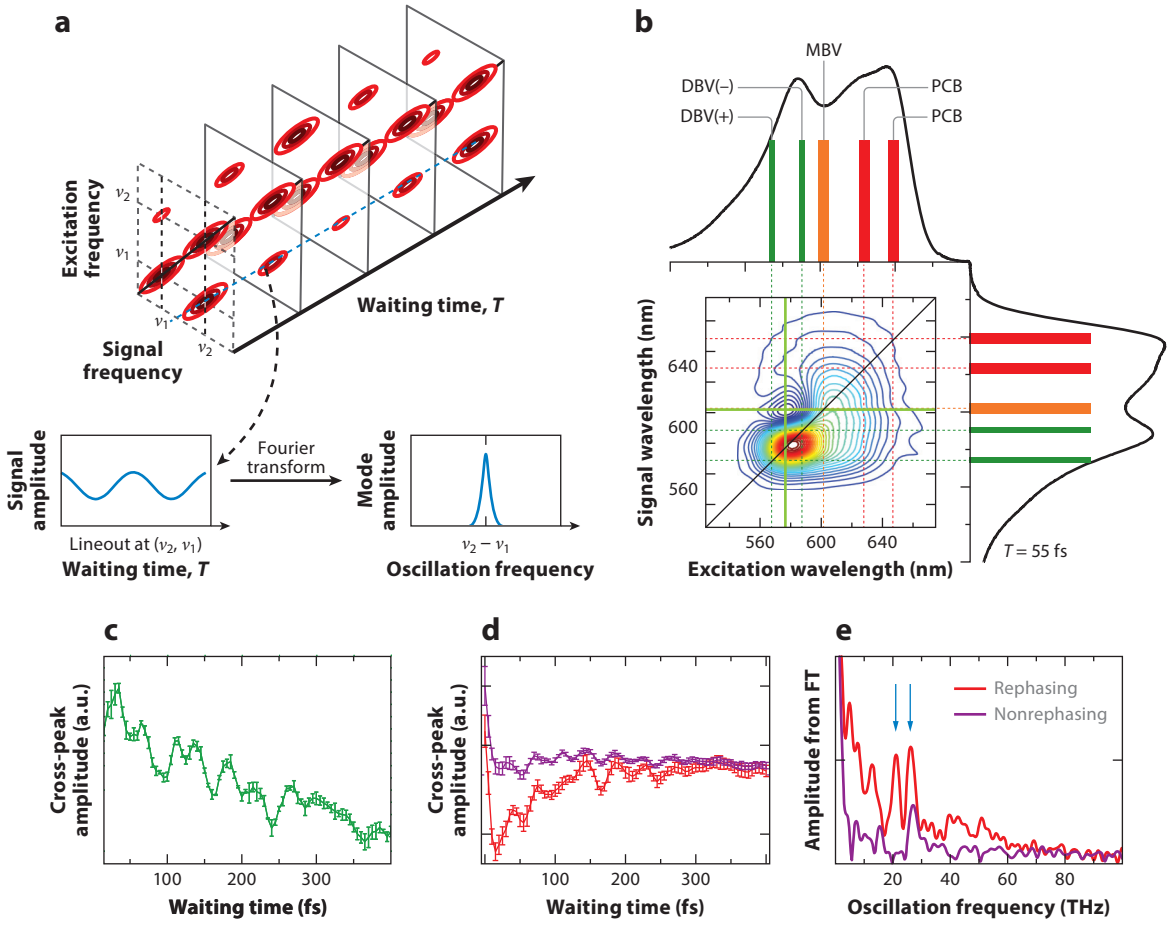

Figure 6

(*a*) Evolution of the 2D spectrum of an idealized dimer system with the waiting time, T. The amplitudes of the cross peaks oscillate at the difference frequency of the two states. A Fourier transform of the signal amplitude at a cross peak gives the oscillation frequency (86). (*b*) A representative 2D spectrum for PC645 at $T = 55$ fs (real part of the total signal). The colored bars in the absorption spectra indicate locations of the estimated peak transition energies of chromophore absorptions, color-coded to match the structure shown in **Figure 2** (40). The cross peak highlighted by the green crosshairs shows a clear coherent oscillation as a function of the pump-probe waiting time. (*c*) Magnitude of the two-dimensional electronic spectroscopy (2DES) amplitude of the (570 nm, 600 nm) cross peak as a function of the waiting time. Error bars indicate one standard deviation as determined from three trials. (*d*) Comparison of (*red*) rephasing and (*purple*) nonrephasing contributions to the (570 nm, 600 nm) cross peak. (*e*) Fourier transformation (FT) of these traces, revealing that the 21-THz frequency is evident only in the rephasing spectrum, whereas the 26-THz frequency is found in both the rephasing and nonrephasing signals (107). Abbreviations: DBV, 15,16-dihydrobiliverdin; MBV, mesobiliverdin; PCB, phycocyanobilin.

for a model dimer system. Two chromophores are strongly electronically coupled. The exciton states are resolved along the diagonal of the 2D spectrum at frequencies ν_1 and ν_2, and also show cross peaks at (ν_1, ν_2) and (ν_2, ν_1) because these excited states share a common ground state; therefore, excitation of one state bleaches the transition of the other.

The short pulse excitation prepares not only populations of the two exciton states, but also superpositions. The signal amplitude of a superposition accumulates phase as a function of pump-probe delay time T and therefore oscillates with a frequency equal to the frequency difference between the states that were coherently excited. Oscillations can appear on the diagonal as well as in cross peaks. In 2007, Fleming and coworkers (20) discovered these kinds of oscillating features in 2DES studies of the Fenna-Matthews-Olson (FMO) protein (at a temperature of 77 K) from green sulfur bacteria. Quite a lot is known about the spectroscopy of the FMO complex, enabling the position of the oscillating cross peak in the 2D spectra to be assigned as a cross peak between two electronic states. On this basis, together with data analysis and modeling, the oscillations were interpreted as electronic coherence. Later work from Engel and coworkers (21) showed a compelling temperature dependence of the decoherence of the oscillations in the FMO 2DES data.

This was a remarkable observation of electronic coherence because of the long timescale that the nonequilibrium exciton coherence survived. We note here that the oscillations themselves are not directly related to EET. They indicate, however, that coherent effects can be present during energy transfer dynamics, therefore motivating the development of new theoretical approaches. Since this first report, our understanding of 2DES signals and the various factors that cause oscillations in 2D maps has vastly improved. Some researchers are predicting ways to distinguish between vibrational and electronic coherences (43, 108–114). The task is challenging, particularly because the 2D spectra of interesting systems are often quite broad and bands are poorly resolved. We discuss this further in the next section.

Figure 6*b*,*c* shows an example of coherent oscillations in 2DES spectra. Three different chromophore types (15,16-dihydrobiliverdin, mesobiliverdin, and phycocyanobilin) provide the primary spectral broadening and establish an energy funnel from the core of the complex (115). Previous modeling of PC645 spectroscopy suggests that the absorption bands are positioned approximately where the colored lines are located in **Figure 6*b*** (116). The representative total, real 2DES spectrum also shown in **Figure 6*b*** displays numerous features of interest, most distinctly an off-diagonal cross peak at (570 nm, 600 nm). Clear coherent oscillations are seen as a function of the pump-probe waiting time (22, 117). Analysis of the 2DES spectrum decomposed into rephasing and nonrephasing contributions (see Section 4.3 and **Figure 6*d*,*e***) (109), comparison with a model protein (118), and comparison with cryptophyte antenna proteins that do not contain the exciton dimer (40) together support the conclusion that the coherent oscillations in the PC645 2DES spectrum at least partially result from electronic coherence.

A central biological question is whether the presence of long-lived vibronic coherence in light-harvesting proteins results in a selective advantage for the organism. For example, researchers have focused on whether coherence is important for efficient light harvesting. According to our definition in Section 2, coherent transfer necessarily accompanies fast energy transfer rates and therefore efficient energy light harvesting. Nevertheless, how fast energy transfer needs to be depends on the antenna architecture. For example, whereas exciton dimers are ubiquitous in light-harvesting complexes (e.g., LH2, LHCII, PC645), they are conspicuously absent from antenna complexes in the genus *Hemiselmis* cryptophytes (**Figure 2**), with their open form structures discovered by Curmi and coworkers (40). Moreover, this loss of exciton dimers is encoded by the gene via an additional amino acid incorporated into one of the subunits, and it arose from cryptophytes that were already using closed-form antenna systems (and hence strong excitons). Successful light harvesting can clearly be achieved in diverse ways, with or without coherent

molecular excitons delocalized over pairs of chromophores. Nevertheless, this profound switching of the electronic coupling (over an order of magnitude) by a change in structure from open to closed must have some functional significance (40).

4.3. A More Complex Picture of the Coherence Emerges

In our early work interpreting the coherent oscillations in 2DES recorded for PC645 and PE545, the data suggested that cross peaks on the upper and lower diagonals of the rephasing signal oscillate out of phase with each other (22). We misinterpreted that as a signature of electronic coherence. In fact, for pure electronic coherence, the cross peaks should oscillate in phase (77, 108). The phase of the oscillations, moreover, depends on excitation conditions (114) and is not a reliable flag for electronic coherence. Later, with higher-quality data, Turner et al. (109, 117) showed that there are several oscillation frequencies in the PC645 2DES data (**Figure 6*c–e***). Assuming a strong electronic coupling model, they demonstrated in a rigorous (although tedious) analysis of signal contributions that purely electronic coherences should oscillate only on the cross peaks of the rephasing 2DES signal contribution, such as the 21-THz (710-cm^{-1}) oscillation shown in **Figure 6*d*,*e***. Conversely, vibrational coherences will oscillate on both rephasing and nonrephasing cross peaks, such as the 26-THz (860-cm^{-1}) oscillation in the PC645 data (**Figure 6*d*,*e***).

An interesting understanding that has developed is that the oscillations most likely arise from vibrational-electronic mixing (36, 113, 119–123). Jonas and coworkers (120) predicted features in 2DES spectra for a vibronic model dimer and realized that at long population times, the coherent oscillations can be persistent because nonadiabatic vibrational-electronic mixing enables new pathways for producing vibrational coherence in the ground state. Independently, Mančal and coworkers (121, 122) found a similar effect that explains a possible origin of long-lived coherences on the electronic excited manifold and showed how the amplitude of vibrational coherences on both the excited- and ground-state electronic manifold can be enhanced by borrowing transition dipole strength when vibrational energy levels match electronic energy gaps. At the same time, Plenio and coworkers (113, 119) proposed a mechanism by which the lifetime of electronic coherences can be enhanced through recoherence assisted by resonant long-lived vibrational coherence.

These insights help us better understand the remarkable timescale during which coherences are maintained. Additionally, O'Reilly and Olaya-Castro (124) showed that the electronic-vibrational mixing confers truly nontrivial quantum properties through nonequilibrium phonon statistics. Although it is not yet obvious how it influences the dynamics, these findings inspire approaches for witnessing quantum effects during EET, even in these macroscopic light-harvesting systems.

Understanding the interplay between electronic coherence and vibrational motion is a fascinating current research direction in the field. Observations currently discussed at meetings on coherent energy transfer include that the electronic energy gaps in photosynthetic proteins apparently are quite often matched to vibrational frequencies. This evidently could help light harvesting, even if only indirectly by modifying the vibronic band intensities.

5. MODELING THE DYNAMICS OF LIGHT HARVESTING

In this section, we present the various challenges associated with modeling EET in photosynthetic systems. The chromophores (e.g., chlorophyll) are usually described as composing the electronic system, whereas the surrounding protein scaffold as well as lipids in the membrane and surrounding water is usually represented collectively as a homogeneous bath with an infinite number of vibrational degrees of freedom. Each chromophore interacts with its own independent environment. As introduced in Section 2, the electronic coupling strength within the system (among the

various chromophores) relative to the coupling of the system to the bath (chromophore-protein) dictates the dynamics of EET. The prediction of transfer rates and interpretation of experimental data are based on theoretical models that inevitably rely on a number of approximations.

Roughly speaking, all models can be reduced to two-level systems coupled to quantum harmonic oscillators, representing electronic degrees of freedom interacting with either photons (125) or phonons (126). Unfortunately, this model, although simple, is not exactly solvable with a finite number of variables—in fact, very few relevant models are amenable to exact analytic solution.

Upon photoexcitation of a chromophore, the coupled bath is brought out of equilibrium. The bath relaxation timescale relative to that of the excitation transfer is relevant to the system dynamics and dictates whether nonequilibrium phonons can participate in the dynamics. If the bath relaxation time is shorter than the energy relaxation timescale, the bath can be considered to remain at equilibrium (and the Markov approximation applies). Otherwise, memory effects and nonequilibrium processes affect EET (18, 63; for a recent review of quantum non-Markovian process, see 127).

5.1. Beyond the Born-Oppenheimer Approximation

Although the Born-Oppenheimer approximation often works well for the spectroscopy of molecules, it does not always work so well for electronically excited molecular aggregates. This is because it assumes that the energy separation between electronic states is much larger than the vibrational level spacings, a condition that usually does not apply to excitonic states of molecular aggregates. The theory of molecular excitons applies to rigid molecules, in which the total wave functions are constructed from the individual molecule electronic wave functions. However, since the late 1950s, it has been recognized that for a coupled system, two different types of spectra need to be distinguished according to the separability of the electronic and nuclear wave functions (128, 129).

The cases of vibronic excitons are distinguished according to the limiting cases, either (*a*) separability applies to the individual molecules, so vibrations are localized on molecules, or (*b*) separability applies to the entire system, so vibrations are normal modes of the delocalized exciton states. These cases correspond to weak and strong electronic coupling, respectively. It was then suggested that the correct description lies in between these limiting cases (128) so that one of the cases could be used as a zeroth-order solution for a more realistic wave function. Expansions to the intermediate regime from both the weak (129) and strong (130) coupling limit were investigated. These methods do not cover the whole range of coupling if the system is not in its vibrational ground state because the vibrationally excited states on the electronic ground-state manifold influence the spectral response, as was first recognized by McRae (131). Limitations of the one-particle approximation (132), which assumes that all the electronically unexcited molecules are in their vibrational ground state, are presented in References 133 and 134.

5.2. Solving Electronic Energy Transfer Dynamics in the Intermediate Coupling Regime

Although it has long been known that the vibrational degrees of freedom influence molecular spectral properties, the account of their effects in dynamical processes remains an open challenge. Whereas computation of classical molecular dynamics is feasible for relatively large many-body systems, an exact solution of the Schrödinger equation, describing the dynamics of quantum systems, is not available for large systems owing to the exponential scaling of the solution with the number of environmental degrees of freedom. The time-dependent Schrödinger equation can only be solved for systems with very few degrees of freedom, using the multiconfiguration

time-dependent Hartree algorithm, for example (135). In the condensed phase, only a few degrees of freedom are relevant to the subsystem of observation (e.g., reaction coordinate, vibrational mode, or electronic degrees of freedom of the chromophore), and a common approach is to treat the remaining variables as an environment. The challenge resides in accurately accounting for the aspects of bath dynamics that affect the subsystem. Commonly used approaches include (*a*) the generalized quantum master equation, (*b*) the path-integral approach, (*c*) mixed quantum-classical approaches, and (*d*) semiclassical methods. **Figure 7** schematically illustrates a selection of available techniques and their respective limitations, which are described below.

5.2.1. Generalized quantum master equation. From the generalized Liouville quantum master equation, the use of the time-convolution formalism and operator technique leads to the Nakajima-Zwanzig quantum master equation (136, 137) (**Figure 7**). Further developments by Kubo and Tanimura led to the HEOM (66) and a reduced form later proposed by Ishizaki & Fleming (52). This approach provides a formally exact solution (within the assumptions of the model) of the dynamics of a reduced system coupled to a quantum bath. It takes advantage of the Gaussian property of the phonon operators in the exciton-phonon interaction Hamiltonian. Assuming Gaussian fluctuations, the cumulant expansion to second order is a rigorous solution. The bath-induced non-Markovian dissipative dynamics are described by a memory kernel $K(\tau)$. The initial system-bath correlations are often neglected but can be captured by an inhomogeneous term $I(t)$ (not to be confused with the spectral overlap defined earlier in this review).

Although the HEOM is general and formally exact, it faces some issues. First, the set of equations needs to be truncated for numerical simulation. Second, the quantities describing the bath are extremely difficult to evaluate, partly because of their high (exponential) dependency on the projection operator. Furthermore, common approximations assume a weak system-bath coupling and a bath fluctuating faster than the system's relaxation rate. The bath is eventually accounted for in terms of free-bath two-time correlation functions, usually described by the spectral density. For an initially uncorrelated system and bath, this reduces to the Redfield equation of motion, which involves only single-phonon processes (138). However, these approximations cannot account for solvation dynamics nor bath memory effects, which appear to be necessary for an accurate description of the dynamics.

As an alternative to the HEOM, a method treating arbitrary system-bath coupling was developed to evaluate the memory kernel of the generalized quantum master equation (139). This approach also uses two-time correlation functions, but for the entire system instead of just the bath. For a harmonic bath, the total system correlation functions can be numerically exactly evaluated using the quasi-adiabatic propagator path-integral method (140). Exact solution is not available in many-body anharmonic systems (such as liquid solutions), and further approximations are required.

5.2.2. Quantum master equation combined with the polaron transformation. As an alternative to the use of a memory kernel, the quantum master equation has been combined with the polaron transformation (69–72) to model coherent resonant energy transfer with arbitrary spectral densities and interpolate between the weak and strong coupling limit accounting for the effect of nonequilibrium phonons in the system dynamics (see **Figure 7**). The polaron transformation is used when neither the system-bath coupling nor electronic coupling is small. By an appropriate frame rotation, the system and bath are mixed, leaving the fluctuations of the electronic couplings induced by the displaced vibrations small compared to all other energy scales. Treating them as perturbations, one can obtain a time-local second-order quantum master equation that accounts for non-Markovian effects and nonequilibrium phonons (i.e., suitable to model EET in the

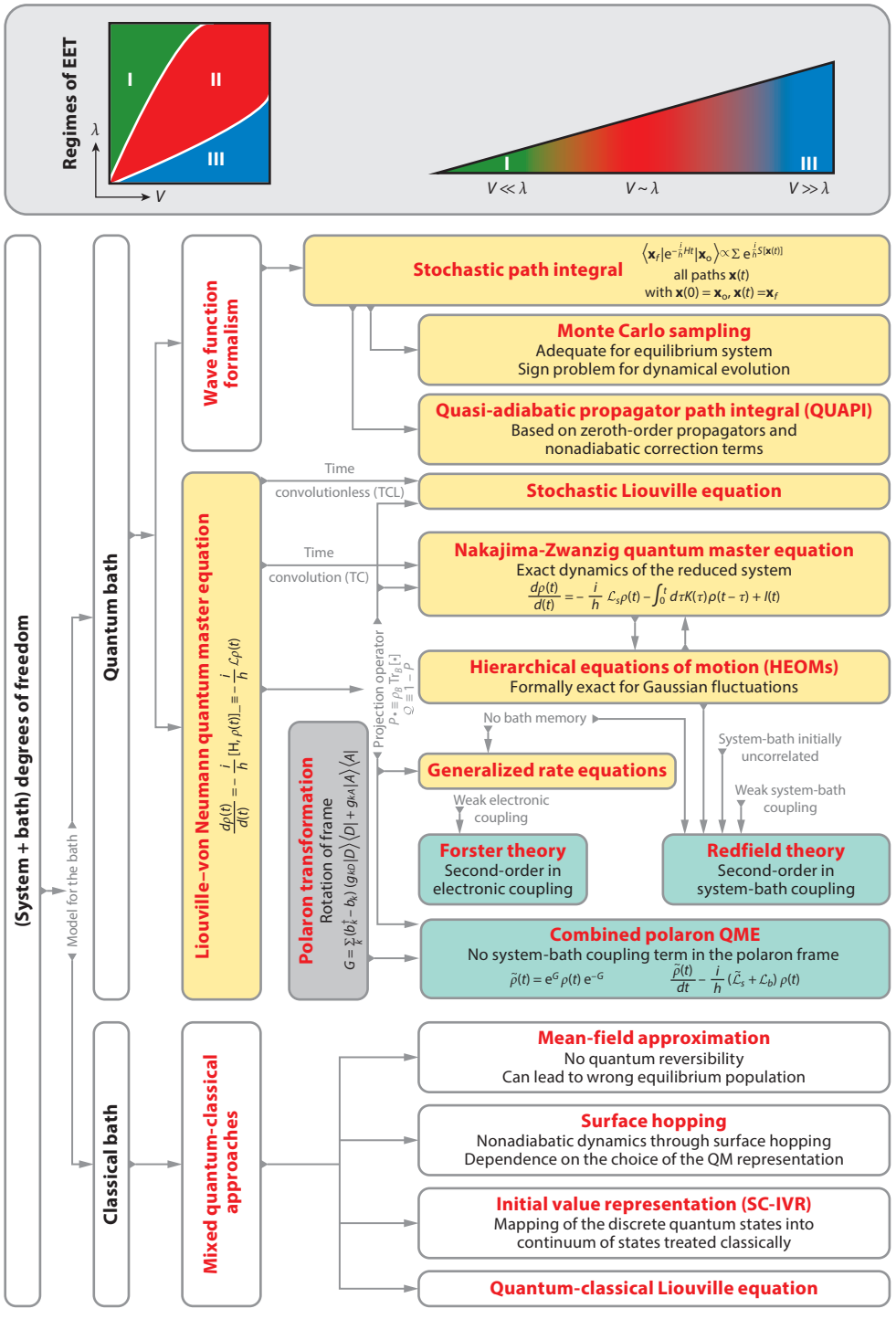

Figure 7

Schematic illustration of a selection of theoretical models available to solve the dynamics of electronic energy transfer (EET) in different coupling regimes. (*Top panel*) Regimes of EET as a function of the bath reorganization energy λ relative to the electronic coupling V (see **Figure 3** for details). Reading the blocks from left to right gives some of the main approximations associated with the different approaches. Nonperturbative (perturbative) models are depicted with a yellow (green) background.

intermediate coupling regime). In this (polaron) frame, both the action of the subsystem on the bath and that of its reciprocal are accounted for in the following way: The effect of the bath on the system appears through renormalization of the electronic couplings and fluctuations owing to their interaction with the vibrational modes; the effect of the system on the bath is reflected through the displacement of the vibrational modes on the electronic excited manifold (141–143).

5.2.3. Path-integral formulation. Instead of using the Schrödinger equation, time-dependent quantum mechanics can also be represented by Feynman's path-integral approach (144). Based on the superposition principle, this method expresses the system dynamics as a sum over the contributions of all possible evolution pathways. Quantum effects in the solvent manifest themselves through nonlocal contributions (i.e., forward and backward paths). Each path, whether classical or quantum mechanical, is equally weighted. The overall contribution of quantum-mechanical paths is generally small because of destructive interferences, and only stationary paths (resulting from constructive interferences) contribute to the final evolution. Unlike the exponential scaling of wave function–based formalisms on the system complexity, Feynman paths are 1D lines independent of the number of degrees of freedom. Resolution remains a numerical challenge. For equilibrium systems, the multidimensional discretized path integral can be evaluated using stochastic Monte Carlo sampling (145). During dynamical simulations, oscillating real-time propagators lead to phase cancellation and failure of the Monte Carlo schemes. Among the various proposed methods (see 146 for a review), the quasi-adiabatic propagator path-integral method is a deterministic approach that provides a successfully converging scheme describing the dynamics of the reference systems in terms of improved propagators (147). Following the idea of the perturbative treatment, propagators are extended from starting-point, zeroth-order propagators. The solution is exact in the case of linear coupling to a harmonic bath, as Gaussian fluctuations can be eliminated exactly. Extension to nonharmonic baths is not straightforward. One model based on forward-backward, semiclassical, initial-value-representation approximation was proposed by Makri & Thompson (148). Alternatively, a numerically exact resolution scheme for nonequilibrium transport was recently developed (149).

5.2.4. Mixed quantum-classical approaches. Often only a few degrees of freedom need to be treated quantum mechanically, and it is appealing, and realistic, to describe the remaining bath degrees of freedom classically. However, because of the different structures of quantum and classical mechanics and the lack of common algebraic structure, consistency between the two descriptions is difficult (150). This is reflected in the general inability of a mixed formalism to predict correct equilibrium distributions at long times. An advantage of quantum-classical methods is that they are easily interfaced with atomistic calculation of the classical fluctuations (e.g., molecular dynamics) (151). Different methods use different strategies for calculating the dynamics based on stochastic trajectories.

Popular quantum-classical models are depicted in **Figure 7**. The surface hopping method is a commonly used approach, first introduced by Tully (152) in the 1970s. All potential energy surfaces are treated classically (with an adiabatic model). Hopping is added phenomenologically to treat the nonadiabatic dynamics and crossing of potential energy surfaces. However, this approach is not invariant to the choice of the quantum representation (diabatic or adiabatic) and destroys the coherence of quantum systems. Nevertheless, we believe the method will be useful for predicting relaxation transitions in molecular excitonic systems, particularly when there is reasonable orbital overlap between the molecules, and dynamics are decided by conical intersections (153).

An alternative approach, proposed by Meyer & Miller (154) and further developed by Stock & Thoss (155), relies on the exact mapping of the discrete quantum variables onto continuous

degrees of freedom, effectively getting rid of the hops between the discrete states. The resulting dynamics are evaluated through a semiclassical initial-value representation of the time-dependent propagator. This approach has proved to be the most adequate semiclassical model for molecular aggregates and to accurately describe the relevant quantum aspects, such as interference and coherent processes (156). An alternative approach consists of solving the mixed quantum-classical Liouville equation (150) and leads to stochastic trajectory algorithms practical for resolution of the dynamics. Makri and coworkers (157) recently developed a path-integral approach for quantum-classical dynamics, which can be more generally used to propagate the density matrix or to evaluate time correlation functions. Alternately, a time-dependent formulation of quantum chemistry—accounting for nonequilibrium effects through the simultaneous resolution of the nuclear dynamics and electronic structure, such as the ab initio multiple spawning method (158)—could be used in future applications to large systems.

6. CONCLUDING REMARKS

Femtosecond spectroscopy, particularly multidimensional spectroscopy, has revealed interesting coherences in photosynthetic light-harvesting complexes. Those experiments do not directly measure coherent energy transfer, but they show that the assumption that excitation is completely localized on chromophores and hops incoherently needs revision. That in turn has motivated incredible advances in theories for electronic energy transfer that capture interesting nonequilibrium and coherence effects. Coherent energy transfer is not simple ballistic or quantum transport in these systems because they are too energetically disordered, nor is it an effect that derives solely from special excitation conditions. Instead, coherent transfer comes from a complicated interplay between dissipation and free evolution giving manifestations of coherence through various processes, including path interferences, system-bath correlations, excitonic delocalization, and non-Markovian phenomena. We argue that those characteristics do matter in photosynthetic light harvesting because they are present in the regime in which energy transfer is fastest. It is not special transport properties conveyed by coherence that are directly significant; rather, it is fast energy transfer that is important for efficient light harvesting.

SUMMARY POINTS

1. Several different physical meanings have been assigned to the word coherence. For the study of photosynthesis, it is appropriate to distinguish among classical coherence (temporal or spectral), quantum coherence (superposition of states), and process coherence (competition between dissipative and free evolution).
2. In photosynthetic complexes, the electronic coupling spans a wide range of values. Large electronic coupling produces molecular excitons, and we designate this as steady-state coherence. Electronic coupling is often the same order as the system-bath interaction. In that case, there is competition between unitary evolution and dissipation, which makes realistic theoretical models difficult to solve. Details of the bath become relevant to theories for EET dynamics.
3. We define coherent EET generally as the regime between the Förster and Redfield limits. Because photosynthetic light harvesting occurs mostly in the intermediate regime between the limiting cases of electronic coupling, coherent transfer matters for light harvesting—it always accompanies the fastest energy transfer.

4. In the coherent regime, superpositions of excitations in the site basis evolve but are maintained on a timescale comparable to the average rate of EET, although there are many subtleties that come into play in various cases.
5. Ultrafast spectroscopy experiments have allowed characterization of the various coupling regimes and have provided new insights into mechanisms of EET in the intermediate coupling regime.
6. Because of the intrinsic mixing between electronic and vibrational degrees of freedom, separation in terms of electronic and vibrational states is not applicable in all coupling regimes. The experimentally observed oscillations reveal a coherent superposition of states that can be of electronic, vibrational, or mixed (vibronic) character.
7. A number of approaches have been developed to model EET dynamics, but photosynthetic complexes present a challenge because of the wide range of coupling regimes and coupling of electronic transitions with intramolecular vibrational transitions.

DISCLOSURE STATEMENT

The authors are not aware of any affiliations, memberships, funding, or financial holdings that might be perceived as affecting the objectivity of this review.

ACKNOWLEDGMENTS

This work was supported by the Natural Sciences and Engineering Research Council of Canada, DARPA (QuBE), and the United States Air Force Office of Scientific Research (FA9550-13-1-0005). A.C. acknowledges the Swiss National Science Foundation (SNSF) for funding and thanks Agata Brańczyk and Paul Brumer for insightful discussions.

LITERATURE CITED

1. Connolly JS, Janzen AF, Samuel EB. 1982. Fluorescence lifetimes of chlorophyll *a*: solvent, concentration and oxygen dependence. *J. Photochem. Photobiol. B. Biol.* 104:142–53
2. Mullineaux CW, Pascal AA, Horton P, Holzwarth AR. 1993. Excitation-energy quenching in aggregates of the LHC II chlorophyll-protein complex: a time-resolved fluorescence study. *Biochim. Biophys. Acta* 1141:23–28
3. Green BR, Parson WW, eds. 2003. *Light-Harvesting Antennas in Photosynthesis*. Dordrecht: Kluwer
4. Sundström V, Pullerits T, van Grondelle R. 1999. Photosynthetic light-harvesting: reconciling dynamics and structure of purple bacterial LH2 reveals function of photosynthetic unit. *J. Phys. Chem. B* 103:2327–46
5. Novoderezhkin V, van Grondelle R. 2010. Physical origins and models of energy transfer in photosynthetic light-harvesting. *Phys. Chem. Chem. Phys.* 12:7352–65
6. van Grondelle R, van Gorkom H. 2014. The birth of the photosynthetic reaction center: the story of Lou Duysens. *Photosynth. Res.* 120:3–7
7. Scholes GD, Fleming GR, Olaya-Castro A, van Grondelle R. 2011. Lessons from nature about solar light harvesting. *Nat. Chem.* 3:763–74
8. Renger T. 2009. Theory of excitation energy transfer: from structure to function. *Photosynth. Res.* 102:471–85
9. Cheng YC, Fleming GR. 2009. Dynamics of light harvesting in photosynthesis. *Annu. Rev. Phys. Chem.* 60:241–62

10. Croce R, van Amerongen H. 2011. Light-harvesting and structural organization of photosystem II: from individual complexes to thylakoid membrane. *J. Photochem. Photobiol. B. Biol.* 104:142–53
11. Blankenship RE. 2002. *Molecular Mechanisms of Photosynthesis*. Oxford: Blackwell
12. Jursinic P, Govindjee. 1977. Temperature dependence of delayed light emission in the 6 to 340 microsecond range after a single flash in chloroplasts. *Photochem. Photobiol.* 26:617–28
13. Wientjes E, van Amerongen H, Croce R. 2013. Quantum yield of charge separation in photosystem II: functional effect of changes in the antenna size upon light acclimation. *J. Phys. Chem. B* 117:11200–8
14. Colbow K. 1973. Energy transfer in photosynthesis. *Biochim. Biophys. Acta* 314:320–27
15. van Grondelle R. 1985. Excitation energy transfer, trapping and annihilation in photosynthetic systems. *Biochim. Biophys. Acta* 811:147–95
16. Vos M, van Grondelle R, van der Kooij FW, van de Poll D, Amesz J, Duysens LNM. 1986. Singlet-singlet annihilation at low temperatures in the antenna of purple bacteria. *Biochem. Biophys. Acta* 850:501–12
17. Anna JM, Scholes GD, van Grondelle R. 2014. A little coherence in photosynthetic light harvesting. *Bioscience* 64:14–25
18. Ishizaki A, Calhoun TR, Schlau-Cohen GS, Fleming GR. 2010. Quantum coherence and its interplay with protein environments in photosynthetic electronic energy transfer. *Phys. Chem. Chem. Phys.* 12:7319–37
19. Ishizaki A, Fleming GR. 2012. Quantum coherence in photosynthetic light harvesting. *Annu. Rev. Condens. Matter Phys.* 3:333–61
20. Engel GS, Calhoun TR, Read EL, Ahn T-K, Mančal T, et al. 2007. Evidence for wavelike energy transfer through quantum coherence in photosynthetic systems. *Nature* 446:782–86
21. Panitchayangkoon G, Hayes D, Fransted KA, Caram JR, Harel E, et al. 2010. Long-lived quantum coherence in photosynthetic complexes at physiological temperature. *Proc. Natl. Acad. Sci. USA* 107:12766–70
22. Collini E, Wong CY, Wilk KE, Curmi PMG, Brumer P, Scholes GD. 2010. Coherently wired light-harvesting in photosynthetic marine algae at ambient temperature. *Nature* 463:644–48
23. Scholes GD. 2003. Long-range resonance energy transfer in molecular systems. *Annu. Rev. Phys. Chem.* 54:57–87
24. Förster T. 1965. Delocalized excitation and excitation transfer. In *Modern Quantum Chemistry: Instanbul Lectures. Part III: Action of Light and Organic Crystals*, ed. O Sinanoglu, pp. 93–137. New York: Academic
25. Braslavsky SE, Fron E, Rodriguez HB, San Román E, Scholes GD, et al. 2008. Pitfalls and limitations in the practical use of Förster's theory of resonance energy transfer. *Photochem. Photobiol. Sci.* 7:1444–48
26. Andrews DL. 2008. Mechanistic principles and applications of resonance energy transfer. *Can. J. Chem.* 86:855–70
27. Scholes GD, Curutchet C, Mennucci B, Cammi R, Tomasi J. 2007. How solvent controls electronic energy transfer and light harvesting. *J. Phys. Chem. B* 111:6978–82
28. Renger T, Müh F. 2012. Theory of excitonic couplings in dielectric media: foundation of Poisson-TrEsp method and application to photosystem I trimers. *Photosynth. Res.* 111:47–62
29. Berlman IB. 1973. *Energy Transfer Parameters of Aromatic Compounds*. New York: Academic
30. Krueger BP, Scholes GD, Fleming GR. 1998. Calculation of couplings and energy transfer pathways between the pigments of LH2 by the ab initio transition density cube method. *J. Phys. Chem. B* 102:5378–86
31. Hsu C-P. 2009. The electronic couplings in electron transfer and excitation energy transfer. *Acc. Chem. Res.* 42:509–18
32. Kasha M. 1963. Energy transfer mechanisms and molecular exciton model for molecular aggregates. *Radiat. Res.* 20:55–70
33. Scholes GD, Rumbles G. 2006. Excitons in nanoscale systems. *Nat. Mater.* 5:683–96
34. Bardeen CJ. 2014. The structure and dynamics of molecular excitons. *Annu. Rev. Phys. Chem.* 65:127–48
35. Spano FC. 2010. The spectral signatures of Frenkel polarons in H- and J-aggregates. *Acc. Chem. Res.* 43:429–39
36. Scholes GD, Smyth C. 2014. Perspective: detecting and measuring exciton delocalization in photosynthetic light harvesting. *J. Chem. Phys.* 140:110901
37. Andrews DL, Curutchet C, Scholes GD. 2011. Resonance energy transfer: beyond the limits. *Laser Photon. Rev.* 5:114–23

38. Müh F, Madjet ME, Renger T. 2010. Structure-based identification of energy sinks in plant light-harvesting complex II. *J. Phys. Chem. B* 114:13517–35
39. Cogdell RJ, Gall A, Köhler J. 2006. The architecture and function of the light-harvesting apparatus of purple bacteria: from single molecules to in vivo membranes. *Q. Rev. Biophys.* 39:227–324
40. Harrop SJ, Wilk KE, Dinshaw R, Collini E, Mirkovic T, et al. 2014. Single-residue insertion switches the quaternary structure and exciton states of cryptophyte light-harvesting proteins. *Proc. Natl. Acad. Sci. USA* 111:E2666–75
41. Wilk KE, Harrop SJ, Jankova L, Edler D, Keenan G, et al. 1999. Evolution of a light-harvesting protein by addition of new subunits and rearrangement of conserved elements: crystal structure of a cryptophyte phycoerythrin at 1.63-Å resolution. *Proc. Natl. Acad. Sci. USA* 96:8901–6
42. Wormick JM, Liu H, Moran AM. 2011. Exciton delocalization and energy transport mechanisms in R-phycoerythrin. *J. Phys. Chem. A* 115:2471–82
43. Wormick JM, Miller SA, Moran AM. 2010. Toward the origin of exciton electronic structure in phycobiliproteins. *J. Chem. Phys.* 133:024507
44. Wormick JM, Moran AM. 2011. Vibronic enhancement of exciton sizes and energy transport in photosynthetic complexes. *J. Phys. Chem. B* 115:1347–56
45. Apt KE, Collier JL, Grossman AR. 1995. Evolution of the phycobiliproteins. *J. Mol. Biol.* 248:79–86
46. Huo P, Coker DF. 2011. Theoretical study of coherent excitation energy transfer in cryptophyte phycocyanin 645 at physiological temperature. *J. Phys. Chem. Lett.* 2:825–33
47. Scholes GD, Fleming GR. 2000. On the mechanism of light harvesting in photosynthetic purple bacteria: B800 to B850 energy transfer. *J. Phys. Chem. B* 104:1854–68
48. Beddard GS, Porter G. 1976. Concentration quenching in chlorophyll. *Nature* 260:366–67
49. Watson WF, Livingston R. 1950. Self-quenching and sensitization of fluorescence of chlorophyll solutions. *J. Chem. Phys.* 18:802–9
50. Barros T, Kühlbrandt W. 2009. Crystallisation, structure and function of plant light-harvesting complex II. *Biochim. Biophys. Acta* 1787:753–72
51. Orf GS, Blankenship RE. 2013. Chlorosome antenna complexes from green photosynthetic bacteria. *Photosynth. Res.* 116:315–31
52. Ishizaki A, Fleming GR. 2009. Unified treatment of quantum coherent and incoherent hopping dynamics in electronic energy transfer: reduced hierarchy equation approach. *J. Chem. Phys.* 130:234111
53. Hemelrijk PW, Kwa SLS, van Grondelle R, Dekker JP. 1992. Spectroscopic properties of LHC-II, the main light-harvesting chlorophyll *a/b* protein complex from chloroplast membranes. *Biochim. Biophys. Acta* 1098:159–66
54. Szalay L, Tombácz E, Singhal GS. 1974. Effect of solvent on the absorption spectra and Stokes' shift of absorption and fluorescence of chlorophylls. *Acta Phys. Acad. Sci. Hung.* 35:29–36
55. Scholes GD. 2010. Quantum-coherent electronic energy transfer: Did nature think of it first? *J. Phys. Chem. Lett.* 1:2–8
56. Jumper C, Anna J, Stradomska A, Schins J, Myahkostupov M, et al. 2014. Intramolecular radiationless transitions dominate exciton relaxation dynamics. *Chem. Phys. Lett.* 599:23–33
57. Rebentrost P, Mohseni M, Kassal I, Lloyd S, Aspuru-Guzik A. 2009. Environment-assisted quantum transport. *New J. Phys.* 11:033003
58. Plenio MB, Huelga SF. 2008. Dephasing-assisted transport: quantum networks and biomolecules. *New J. Phys.* 10:113019
59. May V, Kühn O. 2001. *Charge and Energy Transfer Dynamics in Molecular Systems*. Berlin: Wiley-VCH
60. Ishizaki A, Fleming GR. 2009. On the adequacy of the Redfield equation and related approaches to the study of quantum dynamics in electronic energy transfer. *J. Chem. Phys.* 130:234110
61. Nalbach P, Ishizaki A, Fleming G, Thorwart M. 2011. Iterative path-integral algorithm versus cumulant time-nonlocal master equation approach for dissipative biomolecular exciton transport. *New J. Phys.* 13:063040
62. Dijkstra AG, Tanimura Y. 2012. The role of the environment time scale in light-harvesting efficiency and coherent oscillations. *New J. Phys.* 14:073027
63. Rebentrost P, Mohseni M, Aspuru-Guzik A. 2009. Role of quantum coherence and environmental fluctuations in chromophoric energy transport. *J. Phys. Chem. B* 113:9942–47

64. Hossein-Nejad H, Olaya-Castro A, Scholes GD. 2012. Phonon-mediated path-interference in electronic energy transfer. *J. Chem. Phys.* 136:024112
65. Wu J, Cao J. 2013. Higher-order kinetic expansion of quantum dissipative dynamics: mapping quantum networks to kinetic networks. *J. Chem. Phys.* 139:044102
66. Tanimura Y. 2006. Stochastic Liouville, Langevin, Fokker-Planck, and master equation approaches to quantum dissipative systems. *J. Phys. Soc. Jpn.* 75:082001
67. Mülken O, Mühlbacher L, Schmid T, Blumen A. 2010. Dissipative dynamics with trapping in dimers. *Phys. Rev. E* 81:041114
68. Weiss S, Hützen R, Becker D, Eckel J, Egger R, Thorwart M. 2013. Iterative path integral summation for nonequilibrium quantum transport. *Phys. Status Solidi B* 250:2298–314
69. Jang S. 2011. Theory of multichromophoric coherent resonance energy transfer: a polaronic quantum master equation approach. *J. Chem. Phys.* 135:034105
70. Jang S, Cheng Y-C, Reichman D, Eaves J. 2008. Theory of coherent resonance energy transfer. *J. Chem. Phys.* 129:101104
71. Kolli A, Nazir A, Olaya-Castro A. 2011. Electronic excitation dynamics in multichromophoric systems described via a polaron-representation master equation. *J. Chem. Phys.* 135:154112
72. Nazir A, McCutcheon DPS, Chin AW. 2012. Ground state and dynamics of the biased dissipative two-state system: beyond variational polaron theory. *Phys. Rev. B* 85:224301
73. Gardner WA. 1992. A unifying view of coherence in signal processing. *Signal Process.* 29:113–40
74. Glauber RJ. 2007. *Quantum Theory of Optical Coherence*. Berlin: Wiley-VCH
75. Loudon R. 2000. *The Quantum Theory of Light*. New York: Oxford Univ. Press
76. Kassal I, Yuen-Zhou J, Rahimi-Keshari S. 2013. Does coherence enhance transport in photosynthesis? *J. Phys. Chem. Lett.* 4:362–67
77. Brańczyk A, Turner DB, Scholes GD. 2014. Crossing disciplines: a view on two-dimensional optical spectroscopy. *Ann. Phys.* 526:31–49
78. Mančal T, Valkunas L. 2010. Exciton dynamics in photosynthetic complexes: excitation by coherent and incoherent light. *New J. Phys.* 12:065044
79. Brumer P, Shapiro M. 2012. Molecular response in one-photon absorption via natural thermal light versus pulsed laser excitation. *Proc. Natl. Acad. Sci. USA* 109:19575–78
80. Chenu A, Maly P, Mančal T. 2014. Dynamic coherence in excitonic molecular complexes under various excitation conditions. *Chem. Phys.* 439:100–10
81. Porter G. 1978. The Bakerian Lecture, 1977: in vitro models for photosynthesis. *Proc. R. Soc. Lond. A* 362:281–303
82. Jonas DM. 2003. Two-dimensional femtosecond spectroscopy. *Annu. Rev. Phys. Chem.* 54:425–63
83. Brixner T, Mančal T, Stiopkin IV, Fleming GR. 2004. Phase-stabilized two-dimensional electronic spectroscopy. *J. Chem. Phys.* 121:4221–36
84. Abramavicius D, Palmieri B, Voronine DV, Sanda F, Mukamel S. 2009. Coherent multidimensional optical spectroscopy of excitons in molecular aggregates: quasiparticle versus supermolecule perspectives. *Chem. Rev.* 109:2350–408
85. Cho MH, Vaswani HM, Brixner T, Stenger J, Fleming GR. 2005. Exciton analysis in 2D electronic spectroscopy. *J. Phys. Chem. B* 109:10542–56
86. Fassioli F, Dinshaw R, Arpin PC, Scholes GD. 2014. Photosynthetic light harvesting: excitons and coherence. *J. R. Soc. Interface* 11:20130901
87. Heller E. 1981. A semiclassical way to molecular spectroscopy. *Acc. Chem. Res.* 14:368–75
88. Gruebele M, Zewail A. 1993. Femtosecond wave packet spectroscopy: coherences, the potential, and structural determination. *J. Chem. Phys.* 98:883–902
89. Bardeen CJ, Wang Q, Shank CV. 1995. Selective excitation of vibrational wave packet motion using chirped pulses. *Phys. Rev. Lett.* 75:3410–13
90. Fleming GR. 1986. *Chemical Applications of Ultrafast Spectroscopy*. New York: Oxford Univ. Press
91. Banin U, Bartana A, Ruhman S, Kosloff R. 1994. Impulsive excitation of coherent vibrational motion ground surface dynamics induced by intense short pulses. *J. Chem. Phys.* 101:8461–81
92. Vos MH, Rappaport F, Lambry J-C, Breton J, Martin J-L. 1993. Visualization of coherent nuclear motion in a membrane protein by femtosecond spectroscopy. *Nature* 363:320–25

93. Vos MH, Jones MR, Hunter CN, Breton J, Martin J-L. 1994. Coherent nuclear dynamics at room temperature in bacterial reaction centers. *Proc. Natl. Acad. Sci. USA* 91:12701–5
94. Chachisvilis M, Fidder H, Pullerits T, Sundström V. 1995. Coherent nuclear motions in light-harvesting pigments and dye molecules, probed by ultrafast spectroscopy. *J. Raman Spectrosc.* 26:513–22
95. Monshouwer R, Baltuska A, van Mourik F, van Grondelle R. 1998. Time-resolved absorption difference spectroscopy of the LH-1 antenna of *Rhodopseudomonas viridis*. *J. Phys. Chem. A* 102:4360–71
96. Bradforth SE, Jimenez R, van Mourik F, van Grondelle R, Fleming GR. 1995. Excitation transfer in the core light-harvesting complex (LH1) of *Rhodobacter sphaeroides*: an ultrafast fluorescence depolarization and annihilation study. *J. Phys. Chem. B* 99:16179–91
97. McClure SD, Turner DB, Arpin PC, Mirkovic T, Scholes GD. 2014. Coherent oscillations in the PC577 cryptophyte antenna occur in the excited electronic state. *J. Phys. Chem. B* 118:1296–308
98. Pollard WT, Dexheimer SL, Wang Q, Peteanu LA, Shank CV, Mathies RA. 1992. Theory of dynamic absorption spectroscopy of nonstationary states. 4. Application to 12-fs resonant impulsive Raman spectroscopy of bacteriorhodopsin. *J. Phys. Chem.* 96:6147–58
99. Braun M, Sobotta C, Dürr R, Pulvermacher H, Malkmus S. 2006. Analysis of wave packet motion in frequency and time domain: oxazine 1. *J. Phys. Chem. A* 110:9793–800
100. Jonas DM, Bradforth SE, Passino SA, Fleming GR. 1995. Femtosecond wavepacket spectroscopy: influence of temperature, wavelength, and pulse duration. *J. Phys. Chem.* 99:2594–608
101. Yuen-Zhou J, Krich JJ, Aspuru-Guzik A. 2012. A witness for coherent electronic versus vibronic-only oscillations in ultrafast spectroscopy. *J. Chem. Phys.* 136:234501
102. Tanimura Y, Mukamel S. 1993. Temperature dependence and non-Condon effects in pump-probe spectroscopy in the condensed phase. *J. Opt. Soc. Am. B* 10:2263–68
103. Brixner T, Stenger J, Vaswani HM, Cho M, Blankenship RE, Fleming GR. 2005. Two-dimensional spectroscopy of electronic couplings in photosynthesis. *Nature* 434:625–28
104. Ginsberg NS, Cheng Y-C, Fleming GR. 2009. Two-dimensional electronic spectroscopy of molecular aggregates. *Acc. Chem. Res.* 42:1352–63
105. Cundiff ST, Zhang TH, Bristow AD, Karaiskaj D, Dai XC. 2009. Optical two-dimensional Fourier transform spectroscopy of semiconductor quantum wells. *Acc. Chem. Res.* 42:1423–32
106. Hochstrasser RM. 2007. Two-dimensional spectroscopy at infrared and optical frequencies. *Proc. Natl. Acad. Sci. USA* 104:14190–96
107. Turner DB, Dinshaw R, Lee K, Belsley MS, Wilk KE, et al. 2012. Quantitative investigations of quantum coherence for a light-harvesting protein at conditions simulating photosynthesis. *Phys. Chem. Chem. Phys.* 14:4857–74
108. Cheng YC, Fleming GR. 2008. Coherence quantum beats in two-dimensional electronic spectroscopy. *J. Phys. Chem. A* 112:4254–60
109. Turner DB, Wilk KE, Curmi PMG, Scholes GD. 2011. Comparison of electronic and vibrational coherence measured by two-dimensional electronic spectroscopy. *J. Phys. Chem. Lett.* 2:1904–11
110. Butkus V, Zigmantas D, Abramavicius D, Valkunas L. 2013. Distinctive character of electronic and vibrational coherences in disordered molecular aggregates. *Chem. Phys. Lett.* 587:93–98
111. Perlik V, Lincoln C, Sanda F, Hauer J. 2014. Distinguishing electronic and vibronic coherence in 2D spectra by their temperature dependence. *J. Phys. Chem. Lett.* 5:404–7
112. Halpin A, Johnson PJM, Tempelaar R, Murphy RS, Knoester J, et al. 2014. Two-dimensional spectroscopy of a molecular dimer unveils the effects of vibronic coupling on exciton coherences. *Nat. Chem.* 6:196–201
113. Plenio MB, Almeida J, Huelga SF. 2013. Origin of long-lived oscillations in 2D spectra of a quantum vibronic model: electronic versus vibrational coherence. *J. Chem. Phys.* 139:235102
114. Christensson N, Milota F, Hauer J, Sperling J, Bixner O, et al. 2011. High frequency vibrational modulations in two-dimensional electronic spectra and their resemblance to electronic coherence signatures. *J. Phys. Chem. B* 115:5383–91
115. Marin A, Doust AB, Scholes GD, Wilk KE, Curmi PMG, et al. 2011. Flow of excitation energy in the cryptophyte light-harvesting antenna phycocyanin 645. *Biophys. J.* 101:1004–13
116. Mirkovic T, Doust AB, Kim J, Wilk KE, Curutchet C, et al. 2007. Ultrafast light harvesting dynamics in the cryptophyte phycocyanin 645. *Photochem. Photobiol. Sci.* 6:964–75

117. Turner DB, Dinshaw R, Lee KK, Belsley MS, Wilk KE, et al. 2012. Quantitative investigations of quantum coherence for a light-harvesting protein at conditions simulating photosynthesis. *Phys. Chem. Chem. Phys.* 14:4857–74
118. Wong CY, Alvey RM, Turner DB, Wilk KE, Bryant DA, et al. 2012. Electronic coherence lineshapes reveal hidden excitonic correlations in photosynthetic light harvesting. *Nat. Chem.* 4:396–404
119. Chin AW, Prior J, Rosenbach R, Caycedo-Soler F, Huelga SF, Plenio MB. 2012. The role of non-equilibrium vibrational structures in electronic coherence and recoherence in pigment-protein complexes. *Nat. Phys.* 9:113–18
120. Tiwari V, Peters WK, Jonas DM. 2013. Electronic resonance with anticorrelated pigment vibrations drives photosynthetic energy transfer outside the adiabatic framework. *Proc. Natl. Acad. Sci. USA* 110:1203–8
121. Chenu A, Christensson N, Kauffmann HF, Mančal T. 2013. Enhancement of vibronic and ground-state vibrational coherences in 2D spectra of photosynthetic complexes. *Sci. Rep.* 3:2029
122. Christensson N, Kauffmann HF, Pullerits T, Mančal T. 2012. Origin of long-lived coherences in light-harvesting complexes. *J. Phys. Chem. B* 116:7449–54
123. Schulze J, Torbjornsson M, Kühn O, Pullerits T. 2014. Exciton coupling induces vibronic hyperchromism in light-harvesting complexes. *New J. Phys.* 16:045010
124. O'Reilly EJ, Olaya-Castro A. 2014. Non-classicality of the molecular vibrations assisting exciton energy transfer at room temperature. *Nat. Commun.* 5:3012
125. Jaynes ET, Cummings FW. 1962. Comparison of quantum and semiclassical radiation theories with application to the beam maser. *Proc. IEEE* 51:89–109
126. Fulton RL, Gouterman M. 1961. Vibronic coupling. I. Mathematical treatment for two electronic states. *J. Chem. Phys.* 35:1059–71
127. Rivas AH, Susana F, Plenio Martin B. 2014. Quantum non-Markovianity: characterization, quantification and detection. *Rep. Prog. Phys.* 77:094001
128. Simpson WT, Peterson DL. 1957. Coupling strength for resonance force transfer of electronic energy in van der Waals solids. *J. Chem. Phys.* 26:588–93
129. McClure DS. 1958. Energy transfer in molecular crystals and in double molecules. *Can. J. Chem.* 36:59–71
130. McRae EG. 1961. Molecular vibrations in the exciton theory for molecular aggregates. I. General theory. *Aust. J. Chem.* 14:329–43
131. McRae EG. 1963. Molecular vibrations in the exciton theory for molecular aggregates. IV. Excited states of weakly-coupled systems. *Aust. J. Chem.* 16:295–314
132. Philpott MR. 1971. Theory of coupling of electronic and vibrational excitations in molecular crystals and helical polymers. *J. Chem. Phys.* 55:2039–54
133. Spano F. 2010. The spectral signatures of Frenkel polarons in H- and J-aggregates. *Acc. Chem. Res.* 43:429–39
134. Basinskaite E, Butkus V, Abramavicius D, Valkunas L. 2014. Vibronic models for nonlinear spectroscopy simulations. *Photosynth. Res.* 121:95–106
135. Meyer H-D, Manthe U, Cederbaum L. 1990. The multi-configurational time-dependent Hartree approach. *Chem. Phys. Lett.* 165:73–78
136. Nakajima S. 1958. On quantum theory of transport phenomena: steady diffusion. *Prog. Theor. Phys.* 20:948–59
137. Zwanzig R. 1966. Approximate eigenfunctions of Liouville operator in classical many-body systems. *Phys. Rev.* 144:170–77
138. Yang M, Fleming GR. 2002. Influence of phonons on exciton transfer dynamics: comparison of Redfield, Förster, and modified Redfield equations. *Chem. Phys.* 275:355–72
139. Zhang ML, Ka BJ, Geva E. 2006. Nonequilibrium quantum dynamics in the condensed phase via the generalized quantum master equation. *J. Chem. Phys.* 125:044106
140. Makri N. 1995. Numerical path integral techniques for long time dynamics of quantum dissipative systems. *J. Math. Phys.* 36:2430–57
141. Rackovsky S, Silbey R. 1973. Electronic energy transfer in impure solids I. Two molecules embedded in a lattice. *Mol. Phys.* 25:61–72

142. Nazir A. 2009. Correlation-dependent coherent to incoherent transitions in resonant energy transfer dynamics. *Phys. Rev. Lett.* 103:146404
143. Kolli A, O'Reilly EJ, Scholes GD, Olaya-Castro A. 2012. The fundamental role of quantized vibrations in coherent light harvesting by cryptophyte algae. *J. Chem. Phys.* 137:174109
144. Feynman RP, Hibbs AR. 1965. *Quantum Mechanics and Path Integrals*. New York: McGraw-Hill
145. Berne BJ, Thirumalai D. 1986. On the simulation of quantum systems: path integral methods. *Annu. Rev. Phys. Chem.* 37:401–24
146. Makri N. 1999. Time-dependent quantum methods for large systems. *Annu. Rev. Phys. Chem.* 50:167–91
147. Makri N. 1992. Improved Feynman propagators on a grid and non-adiabatic corrections within the path integral framework. *Chem. Phys. Lett.* 193:435–45
148. Makri N, Thompson K. 1998. Semiclassical influence functionals for quantum systems in anharmonic environments. *Chem. Phys. Lett.* 291:101–9
149. Segal D, Millis A, Reichman D. 2010. Numerically exact path-integral simulation of nonequilibrium quantum transport and dissipation. *Phys. Rev. B* 82:205323
150. Kapral R. 2006. Progress in the theory of mixed quantum-classical dynamics. *Annu. Rev. Phys. Chem.* 57:129–57
151. Huo P, Bonella S, Chen L, Coker DF. 2010. Linearized approximations for condensed phase non-adiabatic dynamics: multi-layered baths and Brownian dynamics implementation. *Chem. Phys.* 370:87–97
152. Tully JC. 1990. Molecular dynamics with electronic transitions. *J. Chem. Phys.* 93:1061–71
153. Settels V, Schubert A, Tafipolski M, Liu WL, Stehr V, et al. 2014. Identification of ultrafast relaxation processes as a major reason for inefficient exciton diffusion in perylene-based organic semiconductors. *J. Am. Chem. Soc.* 136:932–37
154. Meyer H-D, Miller WH. 1979. A classical analog for electronic degrees of freedom in nonadiabatic collision processes. *J. Chem. Phys.* 70:3214–23
155. Stock G, Thoss M. 1997. Semiclassical description of nonadiabatic quantum dynamics. *Phys. Rev. Lett.* 78:578–81
156. Miller WH. 2012. Perspective: quantum or classical coherence? *J. Chem. Phys.* 136:210901
157. Lambert R, Makri N. 2012. Quantum-classical path integral. I. Classical memory and weak quantum nonlocality. *J. Chem. Phys.* 137:22A552
158. Ben-Num B, Quenneville J, Martínez TJ. 2000. Ab initio multiple spawning: photochemistry from first principles quantum molecular dynamics. *J. Phys. Chem. A* 104:5161–75

Annual Review of
Physical Chemistry
Volume 66, 2015

Contents

Indexes

Errata

An online log of corrections to *Annual Review of Physical Chemistry* articles may be found at http://www.annualreviews.org/errata/physchem